We are IntechOpen, the world's leading publisher of Open Access books Built by scientists, for scientists

6,900
Open access books available

185,000
International authors and editors

200M
Downloads

Our authors are among the

154
Countries delivered to

TOP 1%
most cited scientists

12.2%
Contributors from top 500 universities



WEB OF SCIENCE™

Selection of our books indexed in the Book Citation Index in Web of Science™ Core Collection (BKCI)

Interested in publishing with us?
Contact book.department@intechopen.com

Numbers displayed above are based on latest data collected.
For more information visit www.intechopen.com



Chapter 12

Graphene-Based Materials Functionalization with Natural Polymeric Biomolecules

Edgar Jimenez-Cervantes Amieva,
Juventino López-Barroso,
Ana Laura Martínez-Hernández and
Carlos Velasco-Santos

Additional information is available at the end of the chapter

http://dx.doi.org/10.5772/64001

Abstract

The use of 2D nanocarbon materials as scaffolds for the functionalization with different molecules has been rising as a result of their outstanding properties. This chapter describes the synthesis of graphene and its derivatives, particularly graphene oxide (GO) and reduced graphene oxide (rGO). Both GO and rGO represent a tunable alternative for applications with biomolecules due to the oxygenated moieties, which allow interactions in a either covalent or non-covalent way. From here, other discussed topics are the biofunctionalization with keratin (KE) and chitosan (CS). The non-covalent functionalization is based primarily on secondary interactions such as van der Waals forces, electrostatics interactions, or π–π stacking formed between KE or CS with graphenic materials. On the other hand, covalent functionalization with KE and CS is mainly based on the reaction among the functional groups present in those biomolecules and the graphenic materials. As a result of the functionalization, different applications have been proposed for these novel materials, which are reviewed in order to offer an overview about the possible fields of application of 2D nanocarbon materials. In a nutshell, the objective of this work is as follows: first, overhaul different aspects about the synthesis of graphene chemically obtained, and second, make a review of different approaches in the functionalization of 2D carbon materials with specific biomolecules.

Keywords: graphene oxide, reduced graphene oxide, reduction, functionalization, covalent, non-covalent, chitosan, keratin

INTECH
open science | open minds

© 2016 The Author(s). Licensee InTech. This chapter is distributed under the terms of the Creative Commons Attribution License (http://creativecommons.org/licenses/by/3.0), which permits unrestricted use, distribution, and reproduction in any medium, provided the original work is properly cited. CC BY

1. Introduction

Carbon is one of the most interesting elements of nature and is one of the primary constituents for the formation of all organic matter. Its capacity to bind to itself in different ways makes carbon a very versatile element, giving rise to a series of structures called allotropes. Some of these carbon forms have attracted great interest in the past few decades due to their small size, in the scale of nanometers, and their very particular shape or dimensionality, which directly affect their chemical and physical properties. Among these carbon nanostructures, graphene (GE) has become an outstanding material presenting a unique set of "superlative" properties such as mechanical, electrical, thermal and electronic characteristics, enlisted in many reports [1–4].

Graphene is the name of a single layer of carbon atoms arranged in a two-dimensional (2D) crystalline hexagonal lattice, due to the sp^2 hybridization of carbon. Thus, graphene has strong in-plane σ bonds, responsible for its high mechanical strength and flexibility, and it also has weak out-of-plane π bonds responsible for its thermal carrying, electrical charge, and transparency, and graphene is also impermeable. Nevertheless, all these properties are only observed in a single defect-free graphene layer, which is costly to produce in a scalable degree. Alternatively, there are other ways to produce graphene with relative ease, such as the chemical phase exfoliation of graphite oxide. This method yields the synthesis of graphene oxide (GO), a highly oxidized version of graphene. The subsequent reduction in the oxygen content brings a partial restoration to graphenic state, producing reduced graphene oxide (rGO) or chemically converted graphene (CCG) (**Figure 1a**). These graphene-based materials

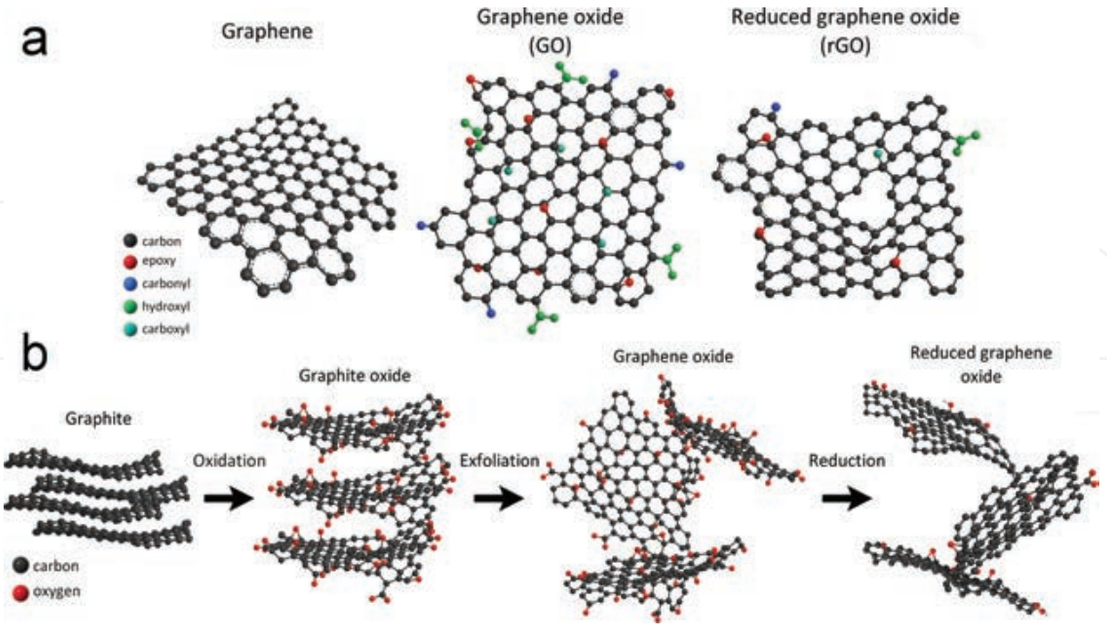


Figure 1. (a) Schematic chemical structures of graphene, graphene oxide, and reduced graphene oxide. (b) Route of graphite to reduce graphene oxide.

are considered as a functionalization of a graphene sheet, because of the presence of oxygen species [5].

Even when GO and rGO have a lower set of properties compared with those of GE, they can be improved through an additional functionalization among others with organic and different bio-molecules. Since the presence of oxygen groups is greater in GO, its reactivity is higher compared with rGO, and thus, graphene oxide is more suitable to be functionalized through covalent interactions. On the other hand, even when rGO retain some oxygen sites, its partial graphitic surface makes it adequate for a non-covalent functionalization. In this manner, tailored-made properties can be successfully achieved giving rise to a wide range of potential applications.

In this manner, GO and rGO have been modified with all kind of biomolecule groups, such as nucleic acids, proteins and peptides, antibodies, enzymes, polysaccharides and amino acids, for applications related to biological/biomedical fields which require a good degree of compatibility, adherence, or biocide characteristics. Long-chain biopolymers containing amino groups, such as keratin (a protein) and chitosan (a polysaccharide), show an excellent covalent linkage with GO, and a good adsorption on rGO (keratin), and they could function either increasing the bacterial adhesion or inhibiting the bacterial growth. This chapter focuses in the study and insight of the interactions between amine-containing biopolymers through covalent and non-covalent interactions with GO and rGO. The details of synthesis of graphene oxide and reduction are reviewed and discussed; a brief discussion involving the different types of functionalization is mentioned; finally, some researches related to functionalization of biomolecules on graphenic materials along with their diverse potential uses is also discussed.

2. Graphene oxide and reduced graphene oxide

As a result of the exceptional properties of graphene, different efforts have been made in order to scale up its mass production. In a brief historically account, one of the first approaches were conducted by Lang in 1975, where few layer graphite was obtained by chemical deposition method. Nevertheless, in those days, the characterization techniques were unable to show what Lang has achieved. More recently in 1999, was reported the mechanical cleavage of highly ordered pyrolytic graphite (HOPG) with atomic force microscopy (AFM) tips, in an attempt to exfoliate a single layer of graphene [1]. Finally, in 2004, Novoselov reported the isolate one layer of graphene through "peeling" many times natural graphite with "Scotch" tape. In this method, the graphite layers are sliced down by mechanical exfoliation until one layer is deposited in a substrate [2]. Despite the effectiveness of this method and the high-quality obtained graphene, this process requires a great deal of time and the amount of the as-produced graphene is not enough for practical applications [3, 4].

A possible solution, in order to obtain graphenic materials in larger amounts, has been found on the graphite oxide route, starting from the modified Hummers method [6], which is based on the introduction of functional groups in graphite layers using a mixture of sulfuric acid and potassium permanganate. The versatility of the method, the excellent dispersion acquired in

different solvents [5], and the possibility of a high yield production, makes the graphite oxide route one of the most promising scalable methods. This process mainly consists of three stages (**Figure 1b**).

First, it is necessary to produce graphite oxide by the oxidative intercalation reaction. In this step, the sp^2 carbon arrangement is disrupted by the introduction of oxygenated functional groups, such as hydroxyl and epoxy in the basal plane and carbonyl and carboxyl at the edges (surroundings). During this process, interlaminar space between graphene sheets is increased two or three times than that of pristine graphite, from 3.34 Å to 5.62 Å [1, 7]. Second, graphene oxide (GO) is produced through exfoliation and dispersion of oxidized graphite. It has been reported that cavitation produced by ultrasonic waves within a fluid (commonly distilled water) produces hot spots with temperatures approximately to 5000°C, high local pressures about 500 atm and rates of heating–cooling of 10^9 K/s [8]. Therefore, water molecules (or polar solvents) can be intercalated in graphite oxide, producing an interlaminar spacing of roughly 1.2 nm [9]. Finally, the third stage consists on reducing or diminishing the oxidation degree of GO, in other words the production of reduced graphene oxide. In terms of recovery thermal, electrical, and mechanical properties, GO has been subjected to a variety of treatments to diminish the oxidized state or the number of oxidized moieties on it. Treatments such as chemical, thermal, UV radiation, and electrochemical reduction have been applied in either individual or multi-steps, partially recovering the sp^2 arrangement found in pristine graphene [6, 7].

2.1. Synthesis of graphene oxide

GO is a covalent carbon structure where at least 60% of its atoms show sp^3 hybridization connected by σ bonds to oxygen atoms, whereas the structure of basal plane is preserved even though it has substantial deformations. Therefore, GO is a hybrid material considered as an insulator exhibiting a resistance about 10^{12} Ω/sq depending on sp^2 and sp^3 formed during oxidation [10]. GO thickness is theoretically within 0.7–0.8 nm because of the oxygenated moieties present on its surface, that is, roughly twice as the thickness of single layer of pristine graphene; however, GO could be larger considering that the occasional presence of bulkier functionalities, organic adsorbates, even some contaminants and so on [11].

Inasmuch as GO is not an stoichiometric material, its structure depends on the oxidizing process, this produces an aromatic disrupted lattice rich in functional groups maintaining arranged zones sp^2 (2–3 nm) within a matrix C–O sp^3 [12], and, for this reason, its chemical structure is difficult to determine. Lerf–Klinowski model based on the evidence obtained through nuclear magnetic resonance (NMR) of graphite oxide describes this material such as randomized of oxidized areas. As a result of oxidation sp^2/sp^3 regions are conformed of aromatic or aliphatic six-membered rings [13]. This model is one of the most accepted in order to describe GO structure. From Lerf–Klinowski model, Gao et al. [14], proposed a new model including the presence of lactole rings of five and six members on the edges besides of carboxyl and carbonyl and hydroxyl, while in the basal plane are found tertiary alcohol esters as well as epoxy and hydroxyl groups.

http://dx.doi.org/10.5772/64001

On the other hand, graphite is considering an inexpensive available material for scalable production of GO; additionally, it can be obtained from either natural or synthetic sources [15], which can be influential over the final properties of GO, as has been reported. Undoubtedly for GO is really important, though not unexpected that the final dimension of the GO sheets obtained is strongly influenced for both the incipient size of graphite flakes and its inherent defects in π-structure in conjunction with the oxidation protocols and exfoliation procedure [16, 17].

The fundamental procedure involved in the synthesis of graphene oxide had originally been developed to oxidize graphite by Brodie in 1859 which used fuming nitric acid (HNO_3) with potassium chlorate $KClO_3$, evolving to the Staudenmaier method where oxidation of graphite was carried out with the addition of sulfuric acid (H_2SO_4) and $KClO_3$ in different parts of the oxidation reaction [18]. Finally, Hummers and Offeman developed the most commonly method derived from Staudenmaier's work, where GO is extensively produced from the oxidation of graphite and the process is completed by a subsequent exfoliation of graphite oxide generally made by ultrasound wave or rapid heating [19]. The reaction takes place when a mixture of potassium permanganate ($KMnO_4$) as strong oxidizing agent is combined with a concentrated H_2SO_4 (Eq. (1)). In terms of the permanganate used as an oxidizing agent, it is generally accepted that the main reactive specie in oxidation of graphite is the dimanganese heptoxide (Mn_2O_7) as can been seen in Eq. (2), not taking into account the changes in the method. Mn_2O_7 can react explosively as long as the temperature raise above 55°C or to come into contact with organic compounds [3, 6].

$$KMnO_4 + H_2SO_4 \rightarrow K^+ + MnO_3^+ + H_3O^+ + 3HSO_4^- \quad (1)$$

$$MnO_3^+ + MnO_4^- \rightarrow Mn_2O_7 \quad (2)$$

Chemical species involved in the synthesis of graphene oxide.

Few years ago, Stankovich et al. [20] reported to obtain chemically modified graphene sheets from complete exfoliation of graphite by Hummers method, due to the van der Waals forces are weakened by the oxygenated moieties formed during the oxidation and the change of graphite to hydrophilic character, the hydration and dispersion in aqueous media can be done to obtain stable colloidal dispersions of GO on water. Additionally, the oxygenated moieties on GO have a negative charge, which grant first a good dispersion as well as stability in some organic solvents, alcohol, and water throughout electrostatic repulsion [17]. Consequently, GO have been used in applications such as sensing, composites, electronic devices, it can not only get well dispersion but also offers a platform for functionalization through chemical reactions such as amidation, esterification, and so on [11, 21]. Additionally, another important feature of GO is its amphiphilicity caused by the heterogeneous distribution of functional groups producing both hydrophobic and hydrophilic domains, having great results in order to interact with other materials such as polymers [11] or creating Pickering emulsions with organic

solvents acting as molecular dispersing agent of materials such as carbon nanotubes (CNT) tuning only the solution pH [22].

Generally, the dispersion of GO is made by ultrasonic waves because is an easy, quick and efficient technique in comparison with the stirring and rapid heating process; however, long periods of sonication can be damaged and reduced the size of GO layers impacting on its properties [6, 7]. Sonication can be followed by centrifugation in order to obtain different lateral sizes on graphene oxide sheets based on density-gradient [17]. Furthermore, salts and ions formed, while the oxidation reaction was carried out are removed [3]. Finally, GO can be reduced in order to recover the initial structure present in graphite, after that, properties such as conductivity can be restored until four times as much as in GO.

2.2. Synthesis of reduced graphene oxide

The sp^2 hybridization loss in GO can be partially restored through the removal of oxygen moieties present on its surface. In this regard, GO has been subjected to the different process of reduction resulting in reduced graphene oxide (rGO). In other words, in rGO, there occurs the formation of percolation pathways between nanometric sp^2 domains disrupted in oxidation reaction of graphite [17]. Therefore, rGO is an important material which has captivated scientific attention for its properties alike to those of pristine graphene that has permitted its use in many potentials applications.

The chemical structure of rGO does not have a specific arrangement regarding oxygenated functionalities distribution and aromatic/aliphatic domains. The remaining oxygen atoms exist as a result of the formation of stable carbonyl and ether groups that cannot be removed without making damage to the basal plane. In addition, another kind of defects found in rGO is the so called Stone–Wales defects (heptagons and pentagons pairs) as well as holes caused by losses of carbon in the form of CO and CO_2 in the reduction process [12]. Nonetheless, properties such as resistivity have important changes after the reduction; values of ≈28.6 kΩ/sq have been reported for rGO [3]. On the other hand, even with an incomplete reduction, rGO produced has some advantages in view, it can be both electrically better than GO and still keeps some functional group reactive sites where further functionalization can be made [23]. Therefore, it is possible that the properties on rGO can be tuned, according with the degree of reduction. Hu et al. highlighted the close relationship between oxidation degree of graphite oxide and defects of rGO. Experimentally, they found that it is possible to obtain rGO with a few amount of defects, first with a relative high oxidation degree and second with low addition of $KMnO_4$ used like oxidizing agent (chemical route) in terms of low addition, defects appeared on edges of graphite [24].

As a result of the reduction process visible changes can be observed, for instance, the brown dispersion of GO turns into a black precipitate due to aromatic restoration and re-agglomeration of the rGO sheets, respectively, as a result of the change from hydrophilic to hydrophobic character after removal of functional groups [16]. Additionally, remarkable differences between GO and rGO have been reported under optical microscopy, while GO is mostly transparent rGO has a very light contrast with the substrate (SiO_2/Si wafer), this reflects the

http://dx.doi.org/10.5772/64001

change from insulator GO to rGO an electrical conductive material [25]. In this regard, for UV–vis spectroscopy, GO shows an absorption peak near 230 nm due to π–π^* plasmon, and a shoulder around 300 nm associated with π–π^* transitions in C=O, while rGO exhibits only an absorption peak between 225 and 275 nm, attributed to a better structural order and more C=C bonds [17]. Another important parameter to take into account is the C/O atomic ratio which is obtained in most cases by X-ray photoelectron spectroscopy, elemental analysis and/or energy dispersive spectroscopy [26]. In this regard, different values have been reported, from 2.2 to 2.7 typically for GO to 10–12 for rGO by chemical reduction, even C/O ratio of 50.2 was reported for reduction under acetylene (C_2H_2) atmosphere [10, 17, 27]. Besides, C/O ratio, electrical conductivity also demonstrates the restoration of sp^2 domains through the formation of percolation pathways after reduction. For GO, values of 10^{-6} S cm^{-1}, characteristic of an insulator material, have been reported, [17], whereas for rGO sheets functionalized with pyrene, a conductivity of 1314 S cm^{-1} has been reported [28]. In addition to these parameters, other characterization techniques, such as NMR, atomic force microscopy (AFM), Raman spectroscopy, transmission electron microscopy (TEM), are also used to reveal the structure and properties of rGO.

One method of reduction of GO is through heating of the samples, also called thermal annealing. This approach is generally employed to exfoliate graphite oxide using gradients of temperature higher than 2000°C/min [29]; for example, it has been reported the use of arc discharge method under hydrogen atmosphere yielding C/O molar ratio of 15–18 and a conduction 10 times higher than the traditional arc discharge method, this can be attributable to the *in situ* elimination and healing during the exfoliation [30]. The exfoliation–reduction can be explained given the CO and CO_2 found within layers of graphite oxide, suffering an abrupt expansion increasing the interlayer distance of GO sheets; moreover, the decomposition of oxygenated moieties also produces high pressure and both are able to overcome the van der Waals forces [10, 29]. McAllister et al. [31] reported the generation of pressures of 40 MPa and 130 MPa at 300 and 1000°C, respectively, based on state equation, this exceeds the value of 2.5 MPa, calculated from Hamaker constant as the pressure necessary to exfoliate GO platelets with interlayer distance approximately of 0.7 nm according to the X-ray Diffraction (XRD) made during the oxidation [31]. However, the rGO sheets obtained are small and wrinkled as a result of both, the release of CO_2 and the removal of functional groups; this can be the main difficulty to scale this method [10].

On the other hand, another important method to reduce GO has been the electrochemical reduction mainly caused by the electron exchange among GO and an electrolyte; this has been performed within a typical electrochemical cell through two different routes [10]. First, a one-step electrochemical approach consisting in a reduction from aqueous colloidal suspension of GO in the presence of buffer electrolyte to produce rGO on the electrode surface. The second, a one- or two-step electrochemical approach performed with thin films of GO deposited on a substrate (electrode) in order to form a GO coated-electrode, and subsequently, this is subjected to electrochemical reduction in a standard three electrode system [32]. C/O ratios from 3.57 to 5.57 have been reported with this technique in addition to be an ecofriendly and controllable method; however, it cannot produce rGO in mass [32, 33]. Other emerging methods to produce

rGO such as solvothermal, photocatalyst, and multistep reduction have been reported [10];notwithstanding, they will not be discussed in this chapter.

In spite of the successful reduction with thermal and electrochemical routes, chemical reduction of GO is the most promising method to scale the production of rGO due to the availability of graphite, the relating ease of processing and the possibility to make modifications to the method in order to obtain high-quality graphene. In this regard, recently Chua et al. [26] make a possible classification of chemical reduction approaches in two categories. The first one called "well-supported" mechanism which consist in chemical reduction through widely known agents used in synthetic chemistry such as aluminum hydride and sodium borohydride, which have a determined mechanism of reaction over specific oxygenated moieties. The second one or "proposed" mechanism consists in reducing agents that have not been used in synthetic chemistry in order to reduce GO; consequently, reaction mechanisms are not well determined.

One of the agents used in "proposed" mechanisms is hydrazine (N_2H_4). Hydroxyl, epoxide, and carbonyl groups are the dominant functionalities. Hydrazine is known to form hydrazone and hydrazides in the combination of carbonyl moieties; however, in GO reduction, only hydrazone is formed by the removal of oxygen. Even, when the mechanism of how reduction is carried out by hydrazine has been widely studied, one of the most accepted is the reduction via nucleophilic substitution proposed by Ruoff and co-workers. In this mechanism, the initial resulting derivative from epoxide opening and hydrazine, an alcohol functional group that releases water, is aminoaziridine, which is finally thermally eliminated in form of diimide, forming at the end a double carbon bond on the graphene surface [20]. In spite of the success of hydrazine in order to yield rGO, its toxicity and dangerous handling have limited its use. This has originated different studies about new reduction agents which not only should be safe but also they need to be ecofriendly.

Owing to the extensive search to scale rGO in a safe and nontoxic manner, "green" and safe reduction agents, take ascorbic acid or plant extracts for instance, have been used. L-ascorbic acid (L-AA) or Vitamin C, as it is commonly known, is an essential nutrient which exhibits antioxidant properties. Gao et al. [34] produced rGO through L-AA as reducing agent, while L-tryptophan was added to stabilize the produced rGO aqueous dispersion by electrostatic repulsion. They proposed a two-step reduction mechanism, first S_N2 nucleophilic reaction and second thermal elimination. Due to electron withdrawing, five-membered ring makes the hydroxyls more acidic that result in dissociation of two protons to form an oxygen anion of L-AA. Subsequently, the reduction could be continued with a back side S_N2 nucleophilic as well as releasing H_2O and formation of intermediate species. Finally, thermal elimination of those precedes the yield of rGO. During the reduction, the L-AA pass through oxidation to dehydroascorbic acid. Later was reported that dehydroascorbic acid can be converted into oxalic and glulуronic acid which can interact with the remaining carboxylic moieties in the periphery of rGO, disrupting π–π interactions between rGO sheets avoiding the restacking and consequent agglomerates [35].

Table 1 (Adapted from Ref. [26]) shows a list of "green" agents for the reduction of GO. Additionally, some recent approaches made with antioxidant agent from plant extracts, high H_2-rich water, potassium carbonate (K_2CO_3), and caffeic acid are included.

http://dx.doi.org/10.5772/64001

Reducing agents	C/O ratio	Conditions	Refs.
Reduction methods with "proposed" mechanisms Nitrogen-containing reducing agents			
Hydrazine	10.3[b]	100°C, 24 h	[26]
Oxygen-containing reducing agents			
Methanol	4.0[b]	100°C, 5 days	[26]
Ethanol	6.0[b]	100°C, 5 days	[26]
Isopropyl alcohol	6.9[b]	100°C, 5 days	[26]
Benzyl alcohol	30[b]	100°C, 5 days	[26]
Hydroquinone	–	RT, 20 h	[26]
L-Ascorbic acid/L-tryptophan/NaOH	–	80°C, 24 h	[26]
L-Ascorbic acid	–	RT, 48 h	[26]
L-Ascorbic acid/NH_3	12.5[a]	95°C, 15 min	[26]
Glucose/NH_3	–	95°C, 1 h	[26]
Dextran/NH_3	–	95°C, 3 h	[26]
Gallic acid	5.3[a]	95°C, 6 h	[26]
Caffeic acid*	7.5[a]	95°C, 24 h	[26]
Amino acid			
L-Cysteine	–	RT, 72 h	[26]
Glycine			[26]
L-Lysine	–	50°C, 9 h	[26]
L-Glutathione	–	50°C, 6 h	[26]
Plant extracts			
Green tea	–	90°C, 2.5 h	[26]
C. esculenta leaf	7.1[b]	RT	[26]
M. ferrea Linn. leaf	6.1[b]	RT	[26]
C. sinensis peel	6.0[b]	RT	[26]
R. damascena	–	95°C, 5.5 h	[26]
Rose water/$NaAuCl_4$	–	95°C, 5 h	[36]
Syzygium aromaticum	–	100°C, 30 min	[37]
Spinacea oleracea	–	100°C, 30 min	[38]
Cinnamomum zeylanicum		Refluxed 45 min	[39]
Asian Red Ginseng		80°C, 10 min	[40]
Microorganisms			
Shewanella	–	Anaerobic, 72 h	[26]

Reducing agents	C/O ratio	Conditions	Refs.
Shewanella	3.1[a]	Aerobic, 60 h	[26]
E. coli culture	–	37°C, 48 h	[26]
E. coli biomass	–	37°C, 72 h	[26]
Baker's yeast/NADPH	5.9[a]	35–40°C, 72 h	[26]
Wild carrots roots	11.9[a]	26°C, 72 h	[26]
Proteins			
Bovine serum albumin/NaOH	–	55–90°C, 3–24 h	[26]
Hormones			
Melatonin/NH_3	–	80°C, 3 h	[26]
Others Green reducing agents			
K_2CO_3	–	90°C, 2 h	[41]
H_2-rich water	6.26[a]	90°C, 3 h	[42]

C/O ratio obtained by [a]X-ray Photoelectron spectroscopy [b]Elemental analysis [c]Energy dispersive spectroscopy

Table 1. Reducing agents for GO toward a green reduction.

3. Functionalization

In spite of, the great potential related to pristine graphene, the fact that it possesses no band gap, it is practically chemically unreactive and it has a poor water dispersibility, have a severe effect limiting its applications in certain fields compared to other well-established materials. Nevertheless, functionalization of graphene-based materials has become one of the main alternatives to address these problems. Graphene derivatives, specifically GO and rGO, could be modified with a wide range of organic or inorganic molecules through chemical or physical functionalization [43]. The availability of different oxygen-containing groups and the presence of sp^2 domains enable these materials to interact with a covalent, non-covalent, and the combination of both interactions with other molecules. This produces hybrids or composite materials with a particular set of properties and potential applications [12], such as the increment in their dispersibility, processability, purification, device fabrication, biocompatibility, band gap modification [44].

As Georgakilas emphasized [43, 45], the presence of several oxygen reactive sites in GO yields a higher covalent reactivity compared with rGO, and thus, GO is frequently chosen as a starting material where molecules will be attached to oxygen atoms. On the other hand, non-covalent functionalization makes use of hydrophobic or π-interactions on the surface or basal plane of the graphenic layer, giving rise to the preference of rGO as a starting material for this approach. Furthermore, the remnant oxygen moieties offer the possibility to form hydrogen bonding,

electrostatic interactions, or the combination of all of them. Although these preferences are not a rule, it could be useful in some cases depending on the type of materials to immobilize [46].

3.1. Covalent functionalization of GO

Covalent modification of GO yields chemical derivatives produced by the next routes, analogous to those obtained with other materials [47]:

1. **Click chemistry**. This type of functionalization is related to a quick joining of small organic units with relative ease and a high efficiency under mild conditions, and in some cases even as a semi-quantitative methodology. One of the best-known reactions is the cycloaddition between an azide and alkyne group catalyzed with Cu. However, there are other reactions different from the azide/alkyne that fits with this click approach [48, 49].

2. **Linker reaction**. In some cases, the use of small functional molecules which aid as a bridge or linkage between the surface of the GO and other materials is required, due to the lack of affinity, or to preserve a functional property specially with some biomolecules, where a direct contact with the surface of the carbon material may produce denaturation as in the case of proteins (enzymes, antibodies) [45, 50].

3. **Direct chemical attachment**. In this route, the oxygen functionalities in GO are directly covalently bound to other molecules with or without the aid of a catalyst. This approach yields a stale and reproducible immobilization of molecules.

3.1.1. Chemical reactions by oxygen moiety

Both, click chemistry and liker reaction are considered as a post-functionalization of graphene oxide. Direct chemical attachment could be briefly explained in terms of the organic chemistry of the oxygen moieties in GO (**Figure 2**), according to Georgakilas [48].

i. Carboxylic acids could react mainly through amidation or esterification.

ii. Hydroxyl groups could react mainly through silanization, silylation, or etherification.

iii. Epoxy groups react mainly through a nucleophilic addition with an amine-containing compound, from small molecules to large polymeric chains, with the subsequent ring opening.

iv. Miscellaneous reactions, frequently in a random way, where two or more oxygen moieties could react with one or more functional groups, as in the case of peptides and proteins which present a rich variety of available reactive groups.

After the functionalization, the remaining unreacted oxygen groups on GO could be removed with a post-reduction chemical reaction to recover some of the graphenic character. This is a very common approach that exploits the dispersibility and chemical properties of GO, while the final material resembles in certain degree to graphene. In fact, in some cases, a partial reduction takes place through the functionalization reaction itself due to the presence of a reducing group (like amines) in the attached molecule or because of the conditions/catalyst

employed. In either case, a covalently functionalized rGO is produced with improved properties such as conductivity, thermal stability, or mechanical properties, although the hydrophilic character is diminished [48].

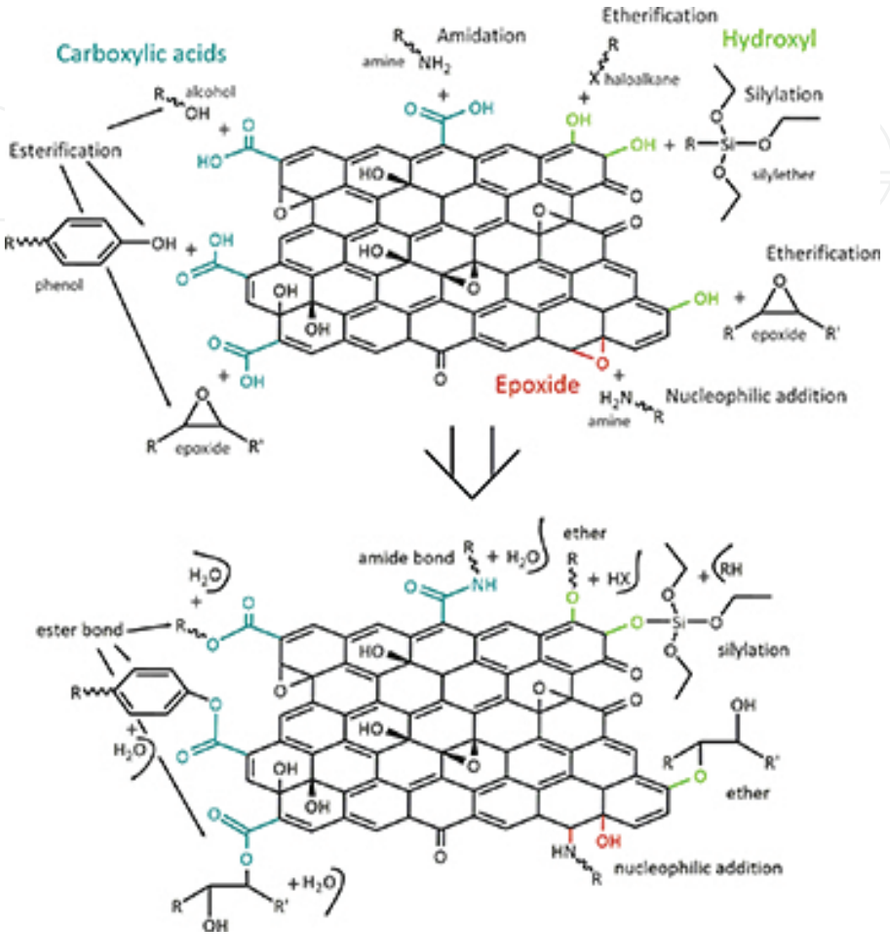


Figure 2. Schematic representation of the covalent functionalization of GO through direct chemical attachment to its oxygen functionalities.

3.2. Non-covalent functionalization of rGO

Unlike the strong covalent functionalization, non-covalent functionalization is an attractive modification route because it offers the possibility to immobilize molecules on both sides of the graphenic basal plane without any further chemical modification of the carbon lattice, avoiding the generation of additional defects, and thus lowering the loss of desired properties, while new properties are introduced [43, 46, 51].

Non-covalent functionalization consists of π-stacking interactions, hydrophobic effects, van der Waals forces, electrostatic interactions, and hydrogen bonding, and in particular situations, even the geometry of the materials plays an important role [52]. In many cases, non-covalent functionalization is accomplished through simple mixing of the materials in an adequate medium [48, 53, 54] or following an incubation protocol for specific biomolecules and cells [55].

As previously mentioned, even though rGO is frequently preferred for this approach, there are many works on the non-covalent modification of GO, followed by a chemical reduction similar to the description above. These non-covalent modifications are usually governed by electrostatic interactions, and thus they depend on the pH of the medium [56–60].

3.2.1. Non-covalent interactions

π interactions occur at the aromatic domains on the surface of both GO and particularly on rGO. π-stacking interactions are fundamental for the stabilization of aromatic systems as in the case of dyes, pyrene functionalized molecules, etc.; aromatic or π-electron-based polymers such as polystyrene, polypyrrol, polyaniline; and biomolecules such as nucleic acids, aromatic residues in polypeptides and some drugs. Such stability is a result of the strong π–π stacking interaction ruled by dispersion forces, not by electrostatic forces. There are other types of π complexes that can be formed with polar gases, cations, and anions. Hydrophobic and van der Waals interactions are exploited by molecules that lack of aromatics or charged groups, such as many polymers, surfactants, quantum dots, and predominantly hydrophobic polypeptides, among others [43, 46, 51].

Oxygen groups such as epoxy and hydroxyl on the surface, and carboxyl and carbonyl at the edges of the layers, allow the adsorption of polar and/or charged molecules through electrostatic interactions and/or the formation of strong hydrogen bonding. While the surface charge of materials is a pH-dependent property, hydrogen bonds is only presented with materials that possesses amine or hydroxyl moieties. Polycationic polymers, polysaccharides, proteins, and enzymes are some examples of molecules, which can present this type of interactions. Even when certain molecules present electrostatic interactions, it can occur that some biomolecules are pH independent, and thus, they are mainly adsorbed due to the hydrophobic or π-interactions [45, 52].

Thus, the combination of the previously discussed non-covalent forces depends on the type of materials and the reaction conditions, and they are very important for the fabrication of new devices [46, 51]. Finally, a common approach consist on the synthesis of systems through the combination of covalent/non-covalent interactions in multiple consecutive stages, yielding very complex hybrid materials or in a multilayer arranged, highly functional, selective, and efficient [46, 61].

Although functionalization of graphene is applicable to very diverse research fields, systems focus on biological applications which represent an attractive and rapidly growing area of research.

4. Functionalization with biomolecules

Even when graphene-based materials have been studied intensively in different fields, their potential in biotechnology and biomedicine applications is still in development, but their research is growing quickly [46]. Graphenic surfaces are ideal to interact with several biomo-

lecules as it has been seen with carbon nanotubes [47, 62]. The combination between graphene materials and biotechnology gives rise to new nano-/bio-interfaces [63] through different biofunctionalization process. Biofunctionalization is defined as the modification of a material by the attachment of biomolecules, ranging from organic groups to very large proteins or even cells. However, biofunctionalization can also be understood in terms of a temporal or permanent biological function as a result of the materials modification [43, 47, 64, 65]. This modification enhances graphene biocompatibility, solubility, immobilization of other molecules, and/or molecular recognition [47, 63].

The different sort of biomolecules could be attached to graphene materials by means of the covalent and non-covalent interactions previously discussed. Notwithstanding, a couple of descriptive examples include the incorporation of nucleic acids and aptamers through π interactions owing to the aromatic character of the nucleobases; the easy assembly of phospholipid chains onto GO and rGO layers through hydrophobic interactions; the immobilization of proteins and enzymes through a combination of hydrophobic and π interactions, and in some cases aided with the contribution of electrostatic forces, in accordance with the amino acid residue composition [46, 51].

Covalently, functionalized graphene biosystems are mainly produced by amidation or esterification reactions of the carboxyl groups, with the aid of coupling reagents or by means of a specific chemical reaction mechanism, although functionalization also includes the epoxy ring opening and hydroxyl modification [46].

Proteins and polysaccharides have the advantage of possessing a rich chemical structure and/or a large amount of functional groups.

4.1. Amine and other functional groups Interactions with graphenic surfaces

Amine functional groups are nucleophiles that possess a basic nitrogen atom with a lone pair. Basically, amines can be classified in primary, secondary, and tertiary, although some cyclic/aromatic amines could be present in certain molecules (tryptophan and histidine in proteins). Nevertheless, amines for chemical graphene modification are frequently found in their primary form, as a pendant or terminated group, whether they are intrinsically present or introduced by chemical modification (amination process).

Amines can react with carboxylic acids of graphene through a condensation reaction forming a stable amide bond. In addition, aminated compounds react through nucleophilic substitution to epoxide groups, yielding an amine addition and a hydroxyl with the ring opening. Chitosan is an excellent example for a macromolecule that can be amide bonded to GO. Also, the N-terminal or amino acid side chain from a protein is commonly reacted through an amide bonding, as well as the lysine residue, or through nucleophilic addition to epoxides. Nonetheless, if the nucleophile is an alcohol (forming an ester with carboxyl groups), a thiol or a carboxylate anion, the variety of reactions becomes larger, just as the non-covalent interactions, as in the case of proteins, such as keratin (KE) among others.

http://dx.doi.org/10.5772/64001

4.2. Keratin functionalization of GO and rGO

Although there are several reports on the usage of proteins, particularly enzymes, for the functionalization of graphene-based materials [46], few works have been done on the surface modification of graphene through the attachment of structural fibrous proteins,[1] and, to the best of our knowledge, only a couple of reports have used keratin [66, 67], specifically, chicken feather keratin, for this purpose.

Fibrous proteins give resistance and flexibility to several biological structures and they possess a high concentration of hydrophobic residues. Keratin is a distinctive fibrous protein compared to collagen, elastin, and myofibril proteins, due to its high degree of disulfide bonds due to the presence of cysteine in its sequence [68]. Keratins are chemically stable and durable against hard environmental conditions; thus, it is found in hair, wool, horns, claws, and feathers.

Chicken feather keratins are small polypeptide chains with a molecular mass of about 10 kDa, and a predominantly hydrophobic character, although it also has a high amount of serine and some other polar or charged groups. It possesses seven cysteine residues, but lacks of lysine, tryptophan, histidine, and methionine. Keratin is therefore adequate for covalent and non-covalent binding with graphene materials.

4.2.1. Covalent attachment of keratin onto GO through a $KMnO_4$ redox system

Redox reaction systems with Mn(III) have been successfully used for the polymerization of vinyl monomers and the grafting of certain macromolecules [66, 69–73]. Mn(III) is obtained from the combination of $KMnO_4$ in acid media with the aid of a reducing reagents, like malic acid, as an electron donor for the reduction of Mn(VII) into Mn(IV) as manganese dioxide. Mn(IV) reacts with the reducing agent to produce the highly reactive Mn(III) ions along with free radicals. This specie can generate active free radicals (primary radicals R) with the reducing reagents, or in the presence of a macromolecule such as a protein, polysaccharide, or graphenic material, yielding a macroradical. These macroradicals may also be formed by the direct attack of primary radicals [74–76].

Keratin and graphene oxide possess different X–H functional groups that may act as electron donors through the abstraction of a hydrogen, thus becoming a radical. In the case of KE, these groups are –SH from cysteine, –OH from serine, threonine, and tyrosine, $–CONH_2$ from glycine and asparagine, and –COOH from glutamic and aspartic acids. In particular, KE also possesses some disulfide bonds (–S–S–) due to the oxidation of thiols. These groups could also be transformed into free radicals with the abstraction of a hydrogen from a neighbor carbon atom [68, 77, 78].

Keratin polypeptide chains are suitable to be grafted onto graphene oxide through a redox reaction system [67]. In this process, keratin needed to be dissolved and dialyzed in order to be chemically attached. Then, under mild conditions in aqueous media and in the presence of sulfuric acid, malic acid, and potassium permanganate, the functionalization was conducted

[1] We are not considering here the case of nanocomposites where graphene materials act as a reinforcement for the polymer matrix.

at two different conditions varying the amount of H_2SO_4/malic acid employed. Keratin polypeptide chains were successfully attached to graphene oxide as it is confirmed by the infrared spectroscopy in **Figure 3a**. The graph shows well-defined peaks from keratin (numbers in red) and graphene oxide (numbers in blue) characteristic vibrations in the covalent bonded materials, and apparently, there is an amide and/or ester bond formation during the reaction, where KE/GO-1 seems to have a higher degree of polypeptide incorporation. In this case, graphene oxide was preferred over reduced GO, due to its higher degree of reactive oxygen sites thus giving a higher yield of chemical bonding.

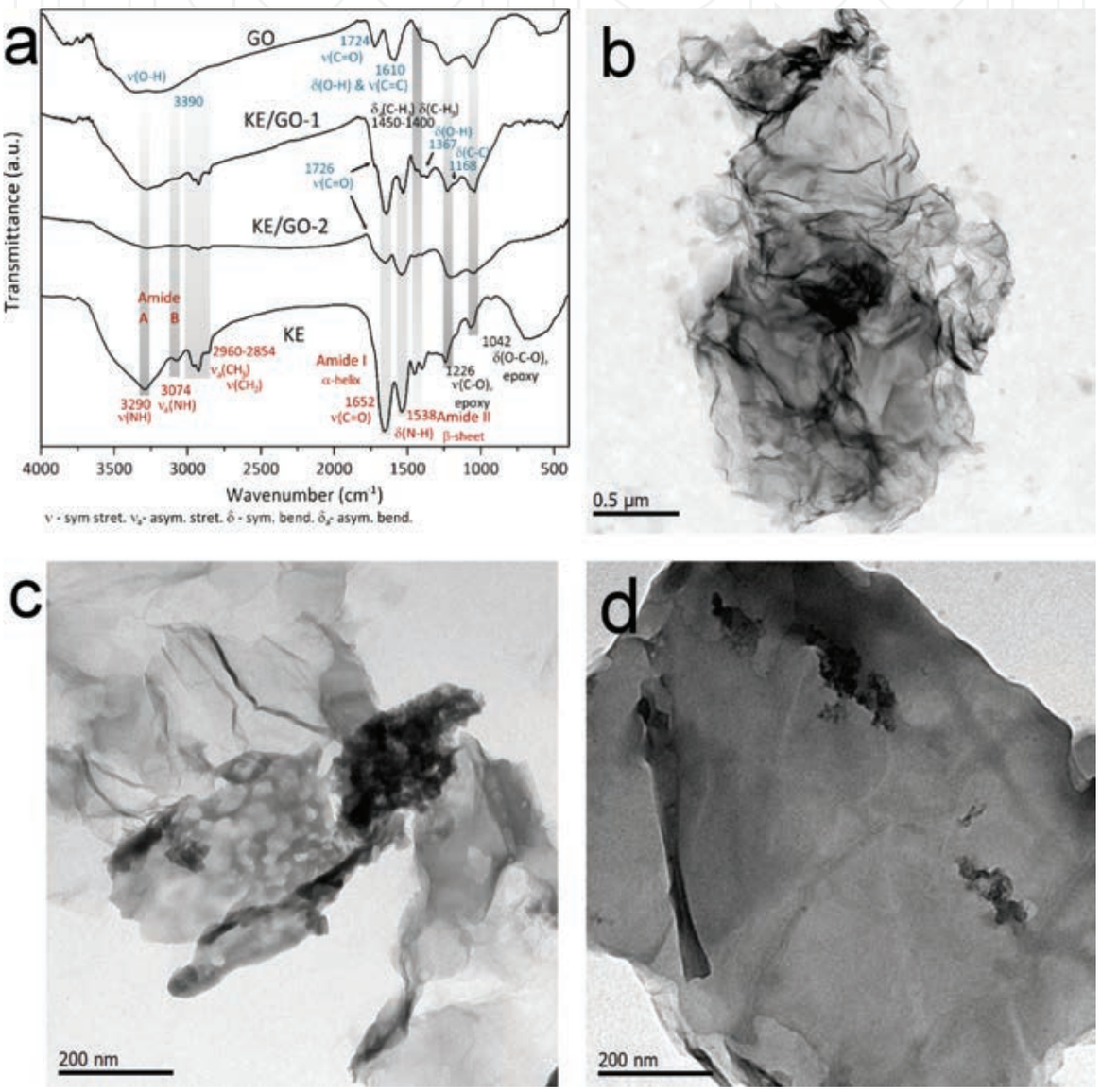


Figure 3. (a) FTIR spectra of graphene oxide, keratin, and the functionalization between them at two conditions (KE/GO-1 and KE/GO-2) and TEM images of (b) GO, (c) KE/GO-1, and (d) KE/GO-2.

Typical TEM image of GO with its intrinsic foldings and wrinkles is shown in **Figure 3b**, where even though the sheets are very large (a couple of microns), they have a very thin structure.

http://dx.doi.org/10.5772/64001

Figure 3c and **d** clearly shows that some morphologies are different than those of the carbon layer sheets, due to the presence of the keratin chains on the surface of the material. To further demonstrate the polypeptide immobilization onto the carbon nanostructure surface, a line-profile chemical composition analysis is also shown in **Figure 4**, confirming the presence of S and N.

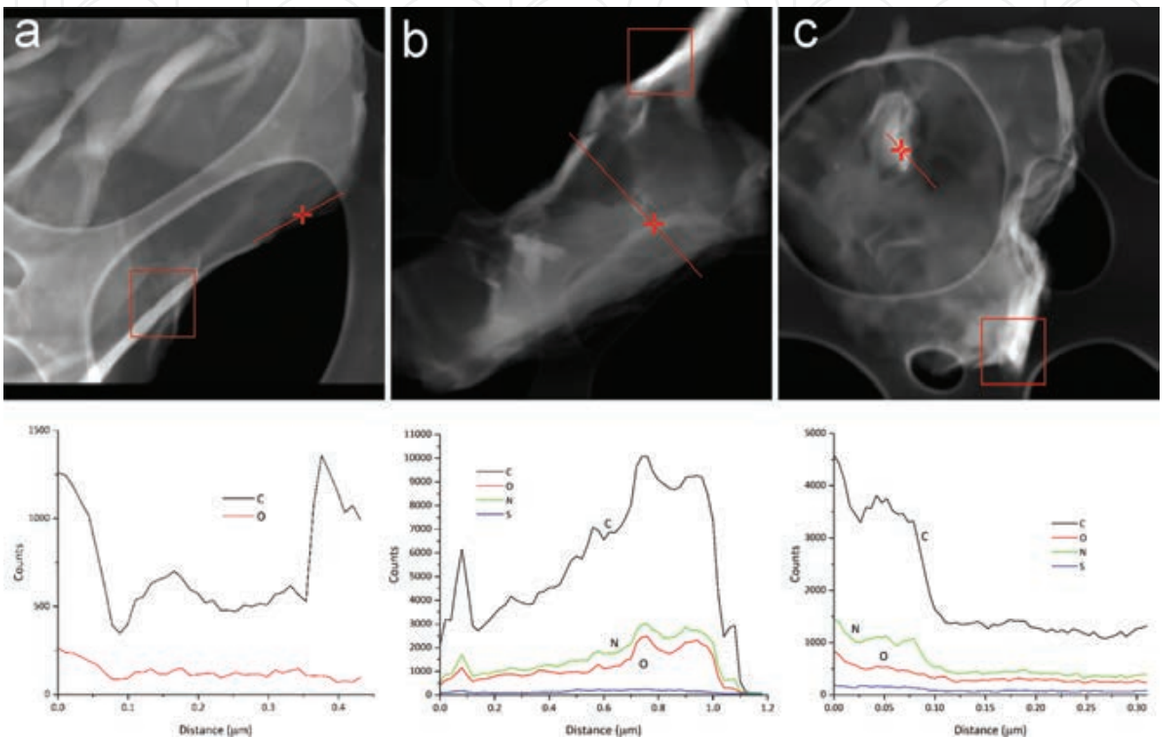


Figure 4. STEM-HAADF images with EDX line scan (red) and chemical profile (below) of (a) GO, (b) KE/GO-1, and (c) KE/GO-2.

4.2.2. Non-covalent attachment of KE onto rGO

Reduced graphene oxide possesses a higher degree of sp^2 hybridization than its graphene oxide counterpart, thus these π-electron domains may interact with hydrophobic or aromatic molecules as well as with aromatic pendant groups, for a non-covalent modification. The oxygen remaining moieties are also useful for an electrostatic- or hydrogen-bonding interactions. In the case of the previously described keratin, the mainly hydrophobic nature of the protein allows its immobilization or adsorption onto the surface of the rGO without the aid of any coupling reagent, while the charged and polar residues could also contribute for the protein tethering forming electrostatic functions depending on the mixing conditions.

Following the procedure for the solubilization of KE, a non-covalent attachment of the protein had been made an aqueous media by simply mixing a KE/rGO mass ratio of 1:1 for 3 h [67]. From the keratin sequence, two amino acids may exhibit:

i. π-stacking: phenylalanine and tyrosine onto the graphene basal plane.

ii. Hydrophobic interaction: proline, glycine valine, cysteine, leucine, isoleucine and alanine, onto both, the basal, and the edges of the layers.

iii. Electrostatic and/or hydrogen bonding: serine, glutamine, threonine, asparagine, glutamic, and aspartic acids.

iv. Strong electrostatic/hydrogen bonding: arginine.

Arginine has a particular strong interaction with negatively charged groups like carboxylic acid, due to its positively charged structure. This residue could be attached to some remaining carboxyl groups in rGO, as it has certainly done in the case of GO [79]. In addition, it is possible that some of the polar residues of the KE will be oriented toward the aqueous media. The effectively non-covalent functionalization of KE onto rGO is indicated by the FTIR spectra of the modified material compared with its precursors (**Figure 5a**).

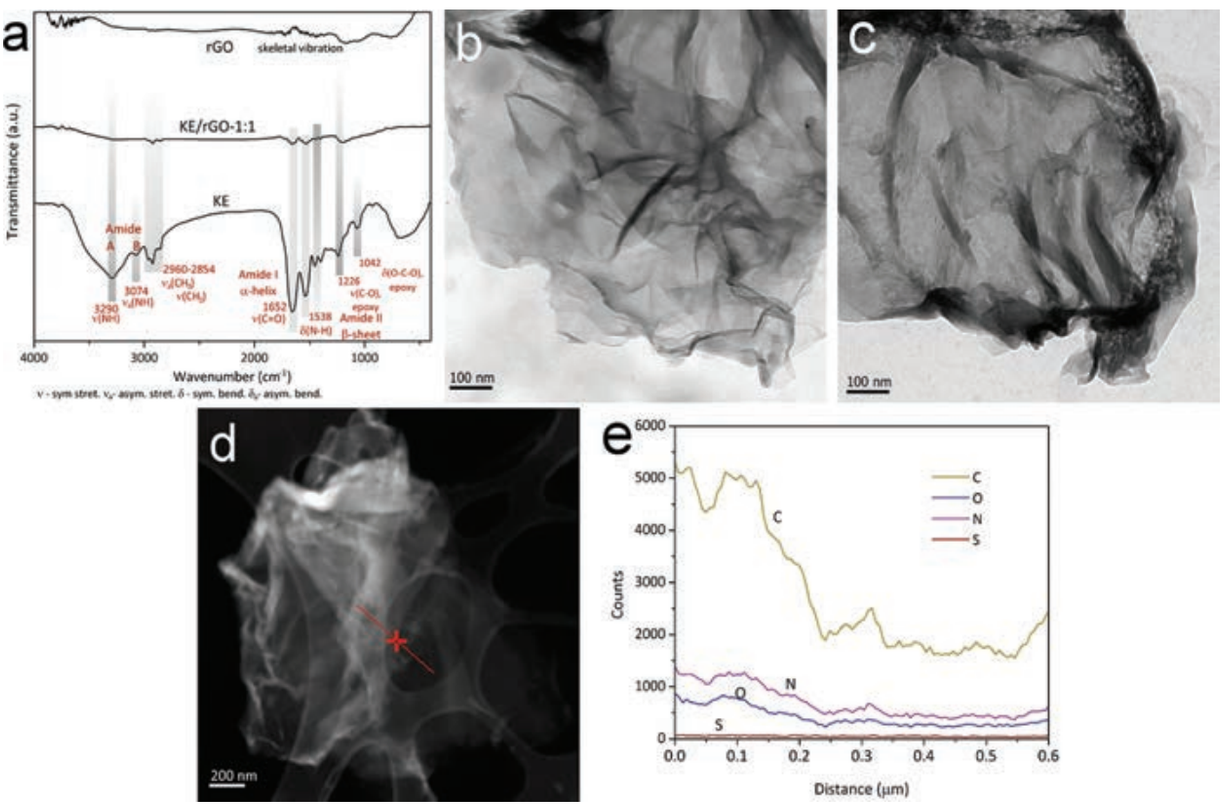


Figure 5. (a) FTIR spectra of reduced graphene oxide, keratin, and the functionalization between them at a mass ratio of 1:1 (KE/rGO-1:1). TEM images of (b) rGO, (c) KE/rGO-1:1, (d) STEM-HAADF images with EDX line scan, and (e) chemical profile of KE/rGO-1:1.

In the same way as with keratin/graphene oxide, transmission electron microscopy and line scan chemical composition had been performed in order to further confirm the functionalization. As can be seen from **Figure 5b** and **c**, a surface roughness besides those intrinsically found

http://dx.doi.org/10.5772/64001

in graphene is appreciated when keratin has been immobilized. Also, chemical compositions clearly show the presence of N and S on the surface of the graphenic layers (**Figure 5d** and **e**).

Based on these results, keratin has an affinity to interact with rGO in a strong manner, practically wrapping the carbon material, even when there is no covalent linkage and no coupling reagents present in the mixture. But there still more future research in order to manipulate the degree or sites of interactions between these two systems

4.3. Chitosan functionalization of GO and rGO

GO and rGO have been functionalized through covalent and non-covalent interactions with several biopolymers; one of them with great relevance due to its potential applications such as tissue engineering, cell adhesion, and food delivery is chitosan (CS) [46]. CS exhibits an unusual combination of properties such as biological activities, mechanical, and physical properties that make it the most important derivative of chitin, the second most abundant natural polysaccharide [80]. CS is composed of β-(1,4)-2-amino-2-deoxy-D-glucose, and it is the result of the deacetylation of chitin (β-(1,4)-2-acetoamido-2-deoxy-D-glucose) [21] which

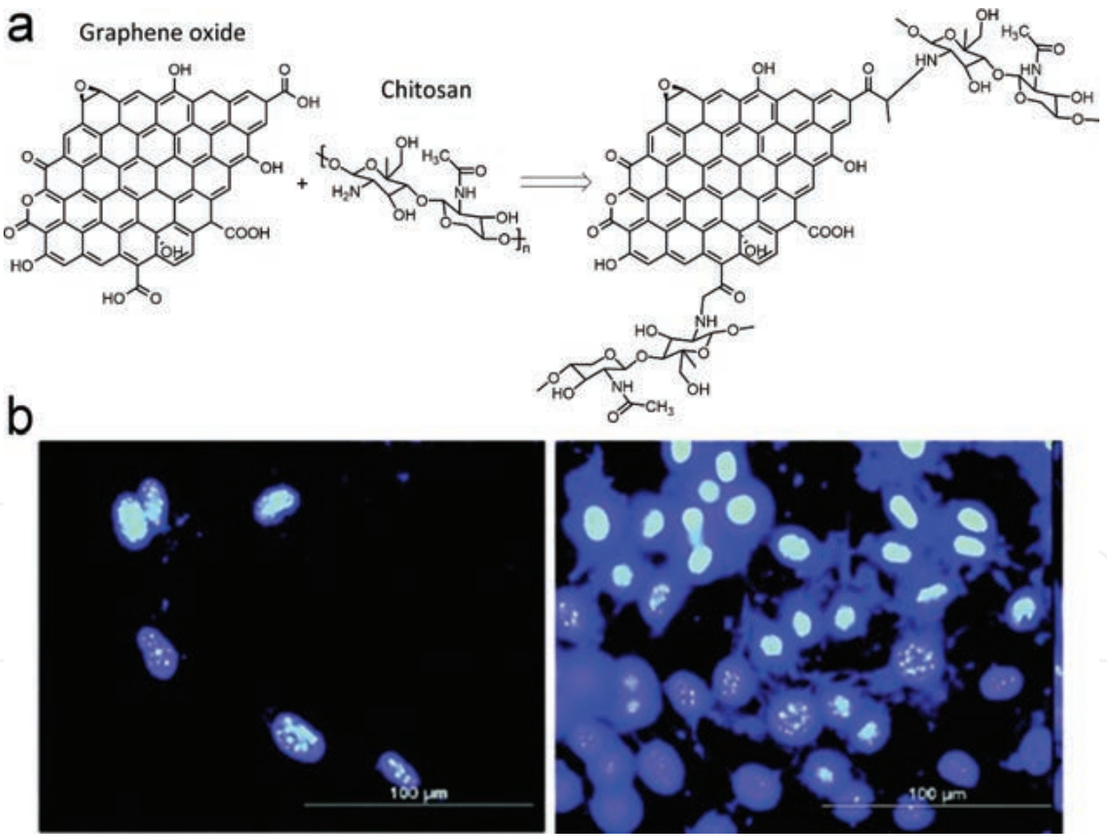


Figure 6. (a) Schematic illustration of covalent interaction between GO and CS trough amide bond formed between –COOH moieties of GO and $–NH_2$ groups, present in CS. (b) Fluorescence micrographs of immunocytochemistry of cell nuclei of pre-osteoblasts after 2 day culture on GO (left) and GO–CS–HAP (right). The graphs shows high fluorescence intensity zones as pre-osteoblasts growth, GO–CS–HAP system has notorious development in comparison to GO. (Adapted from [91] with permission of The Royal Society of Chemistry).

can be found in crustacean shells and shellfish wastes, both of them by-products from marine bioprocessing plants and probably one of the most important sources of CS [81]. CS is a polycationic polymer with two amino and two hydroxyl groups and a carbohydrate backbone similar to cellulose as can be seen in **Figure 6a**. Molecular weight (MW) and degree of deacetylation depend on the alkaline reaction conditions yielding a random distribution of acetylated/deacetylated units coupled in its chains [80]. These two features are chiefly responsible of the physicochemical properties of CS, principally impacting on its biological characteristics [82]. The amino functional groups in CS provide a versatile behavior when CS is in aqueous solution. At low pH (<6), the amino groups are protonated, thus giving CS a polycationic behavior. On the other hand, when pH is higher than 6.5, functional groups in CS are deprotonated, losing its charge and reducing its hydrophilicity [83]. CS is a biocompatible, biodegradable, non-toxic material approved by the FDA; additionally, amino and hydroxyl groups present in its structure offers reactive sites for functionalization; for these reasons, it has been considered together with GO and rGO as a promising material to synthesize new materials for different applications such as biomedical, pharmaceutical, gene therapy, and waste water treatment to mention but a few [80].

4.3.1. Covalent functionalization of GO and rGO with CS

The covalent functionalization of GO and rGO accordingly with reports is made through the interaction between the oxidized moieties on surface of 2D carbon nanomaterial (GO, rGO), and the functional groups present in CS molecule (amino). GO functionalized with CS have been used to developed novel materials via amidation [84], esterification [85], or nucleophilic addition [86, 87]. Esterification was reported by Xu et al., in order to obtain CS grafted onto GO. First GO was dissolved in dimethyl formamide (DMF) in sonication, followed by the addition of thionyl chloride ($SOCl_2$) which reacts with –COOH groups to obtain acyl-chloride functionalized GO (GO–COCl). Finally, $–NH_2$ groups present in chitosan react with GO–COCl via esterification [85]. On the other hand, abundant epoxy groups in GO can react with $–NH_2$ at elevated temperatures following the nucleophilic addition mechanism similar to cross-linking mechanism in epoxy resin during curing [86]. In spite of the successful grafting of CS onto GO via esterification and nucleophilic addition, the most common route to functionalize GO with CS is amidation, which is done by the interaction of –COOH and $–NH_2$ groups present in GO and CS, respectively [84]. GO functionalized with CS (GO–CS) has been used as a scaffold in different fields due to its interesting properties.

Recently, GO–CS system was used as a platform for drug delivery and sensing devices [88–94]. Depan et al. reported a biomimetic mineralization route of conjugated material made up of GO and CS for hydroxyapatite (HAP) biomineralization. HAP as a major component in bones with important features, like great biocompatibility and bioactivity, has been utilized as a part of new multicomponent system (GO–CS–HAP) for bone tissue engineering. The functionalization was completed via covalent modification between highly decorated GO with –COOH moieties and CS with amino groups. Fast Fourier transform infrared spectroscopy (FTIR) in earlier reports of Depan and coworkers showed the formation of amide bond. Prior to functionalization, the characteristic signals of functional groups in CS were observed in 1636

and 1597 cm^{-1} attributed to the stretching of C–O (in –NHCO amide group) and bending of N–H (in $–NH_2$), respectively, whereas for GO grafted with CS, $–NH_2$, signal was shifted to a lower value, while amide group (–NHCO) was shifted to a larger value, this point out that functional groups present in CS and GO interacted to form covalent bonds [95].

On the other hand, HAP nucleation on GO–CS was corroborated by FTIR, X-ray diffraction (XRD) and scanning electron microscopy (SEM). A fine dispersion of HAP was observed, and it was attributed to the electrostatic interactions with GO–CS system which promoted the HAP growth. The adhesion and proliferation of osteoblasts on CS–GO–HAP system was observed in order to evaluate their distribution and attachment, both features are necessary for tissue formation. Samples were analyzed after 1 and 24 h of cells incubation, fluorescence microscopy with DAPI showed a synergistic effect in mineralization of HAP in GO–CS–HAP system as can be seen in **Figure 6b**, attributed to interaction of CS and HAP. Another study about GO functionalized with CS was reported by Mohandes et al., using GO–CS–HAP nanocomposite as a scaffold to grow apatite (AP) due to its high porosity and interconnectivity, both features in nanocomposite are important for the cell attachment and new bone formation. Additionally, thermal stability of GO and GO–CS–HAP was evaluated by termogravimetric analysis which suggests that the loss of mass in GO of approximately 25 wt% is attributed to functional groups, while GO–CS–HAP shows stability at 310°C where the weight loss was important. New AP was formed in GO–CS–HAP nanocomposite after 14 days socked in simulated body fluid (SBF). Grain size of 20–15 nm was observed by scanning electron microscopy (SEM) [96].

Due to its haemostatic properties and safe excretion CS were used to build microneedle arrays as transdermal preloaded drug delivery nanocomposite. Fluorescein sodium (FS) was attached by non-covalent interactions to CS–rGO at the same time reduction of GO was carried out. rGO–CS–FL array shows better mechanical properties and drug release in comparison to pristine CS. Nanocomposite with 2% of rGO achieved maximum release (91%) of available drug in 48 h, while CS–FL system only achieved around 33% according to the report [94]. Other approaches in drug delivery were reported by Rana et al. and Bao et al. The first one reported the use of ibuprofen (IBU) and 5-fluoracil (5-FU) drugs loaded in rGO–CS system via simple physisorption, and additionally, they evaluated the cytotoxicity and cell viability of GO–CS–IBU and GO–CS–5-FU systems over CEM and MCF-7 cancer cells [89]. The second one reported a novel nanocarrier of campthotecin (CPT), an inhibitor of topoisomerase I and anticancer drug. Cell viability of 80% was found in methylthiazoloterazolium (MTT) assay. Additionally, π–π stacking and hydrophobic interactions between GO–CS and CPT allow high load (20 wt %) of drug in nanocarrier [90].

Other approaches regarding removal of contaminants in water have been done. Removal of Cr(IV) from simulated wastewater with magnetic GO–CS ionic liquid (MCGO-IL) was reported with a maximum of 143.35 mg/g of adsorption capacity (Q_{max}), this was described by the Langmuir isotherm. A removal mechanism was proposed. Briefly, first, the electrostatic attraction between Cr(IV) with $–OH_2^+$ and $–NH_3^+$ takes place, second, the cooperation between ionic liquid, functional groups of GO–CS and Cr(IV) occurs and, third, the reduction of Cr(IV) to Cr(III) assisted by π electron of carboxylic six-membered ring in MCGO-IL is achieved [97]. On another report magnetic CS nanoparticles (MCGO) acting as magnetic bioadsorbent shown

to have excellent properties. Magnetic biosorbents can be recovered, easily separated and CS adsorption is better in view of its high surface area along functional groups present [98]. According to Fuschine dye adsorption experiments, pH 5.5 is the optimal value to carry out the removal by MCGO. Moreover, the calculated and experimentally values of adsorption capacity were close, which confirms the pseudo-second-order kinetic model of adsorption proposed. Additionally, the studies over recycling of MCGO as adsorbent shows only slightly decay adsorption capacity of MCGO after the fifth cycle. These results suggested that this method can be used to yield graphene-absorbents in commercial scale. In **Figure 7**, the synthesis of MCGO is briefly represented by a schematic diagram [99].

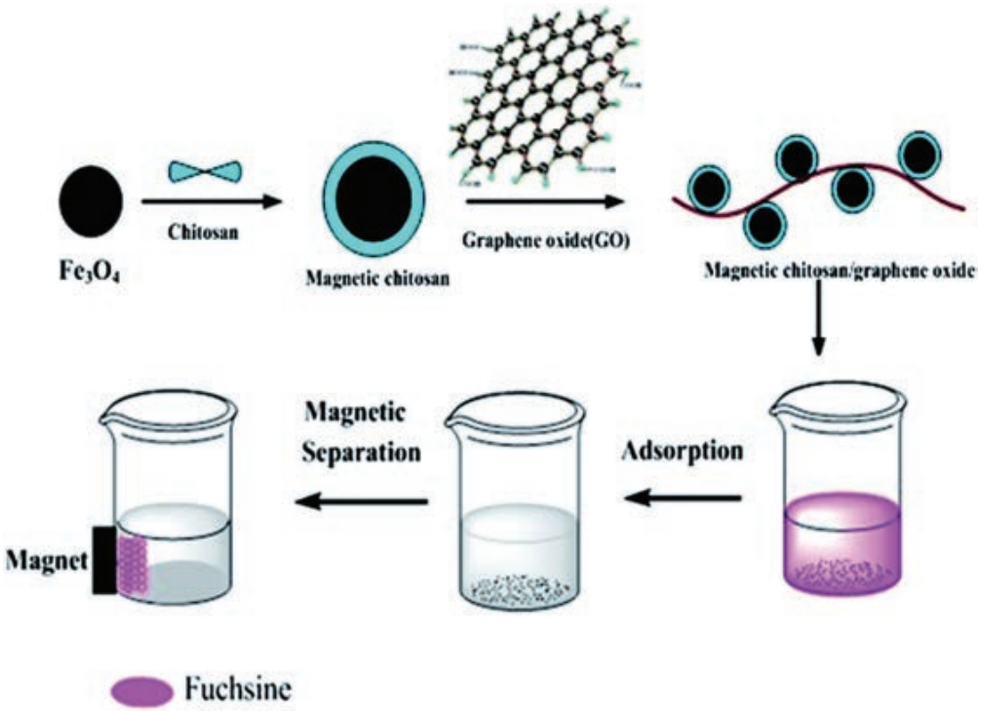


Figure 7. In the synthesis of MCGO, first magnetic particles are attached to CS and second trough amide bond formation GO surface is functionalized. (Reproduced from [99] with permission of The Royal Society of Chemistry).

On the other hand, antifouling membranes were developed by depositing a thin film of GO–CS on polyamide surface to form brackish water thin-film membrane for reverse osmosis (BWTFC-RO). In this approach, the BWTFC-RO with high content of GO shows better antifouling response because of the negative moieties in GO–CS increase hydrophilicity, which can reduced the interfacial energy among membrane surface and water and thus membrane fouling resistance was incremented. A water contact angle of 63.68° was measured for unmodified membrane, while membrane with GO–CS system has a contact angle of 19.13° [100]. In addition, in order to remove Uranium U(vi) released in wastewater, GO–CS systems grafted via covalent were done. Different probes of adsorption and desorption were made having Q_{max} = 225.78 mg/g at pH 4.0 and fitted to a Langmuir model. The removal of U(VI) can

http://dx.doi.org/10.5772/64001

be attributed to interactions between amine groups and the metal; this was corroborated by FTIR where –NHCO– (at 1530 and 1630 cm^{-1}) and $–NH_2$ (at 1420 cm^{-1}) peaks decreased when the U is adsorbed [101].

Owing to the large surface-to-volume ratio and good electrochemical activity of GO and the compatibility of CS, GO–CS nanocomposite enhances transfer electron and DNA immobilization between electrode surface and DNA in electrochemical biosensor for typhoid diagnosis. This was reported using glutaraldehyde (GA) as a bridge between the GO–CS nanocomposite film on indium tin oxide (ITO) electrode and *Salmonella typhi,* specifically its 5′-amine labeled single-stranded DNA (ssDNA). GO–CS–ssDNA–ITO bioelectrode shows improvements in detection limits in comparison to other studies [88], and this is attributed to the excellent conductivity and small band gap from biomolecules; the bioelectrode shows the limits of 100 fM in buffer solution and shelf life of 15 days with a 100% recovery. Otherwise, *Candida rugose* lipase (CRL) immobilization was reported by magnetite particles (Fe_3O_4) assembled in GO–CS system. GO–CS–Fe_3O_4 nanocomposite was synthetized from ferric chloride hexahydrate ($FeCl_3 \cdot 6H_2O$) and 1,6-hexadiamine by solvothermal reaction. The nanocomposite needs only one step to be synthetized which is important when large-scale production can be possible. In this study, three strategies were used to immobilize CRL. Firstly, the electrostatic adsorption by GO–CS–Fe_3O_4, secondly, covalent bonding with GO–CS–Fe_3O_4–GA and thirdly metal-chelate ligand anchorage on GO–CS–Fe_3O_4–IDA-CU. The activity recovery was measured for three systems and the adsorption results showed the best protein CRL immobilization for GO–CS–Fe_3O_4–IDA-CU followed by GO–CS–Fe_3O_4–GA and GO–CS–Fe_3O_4 systems with 65.5, 60.2, and 57.2% of activity recovery, respectively. GO–CS–Fe_3O_4–IDA-CU leads the activity recovery due to exposition of functional groups thus giving low diffuse resistance. On another approach, the biocompatibility of mouse mesenchymalstem C310T1/2 cells adhered to GO–CS covalent attached system was evaluated by DAPI fluorescence, tracing the nucleus of cells and low cytotoxicity was further reported. Additionally, cell viability after 24 h shown low death cell indications. This can be traduced in an acceptable biocompatibility of GO–CS system [93].

Another emergent field of study of GO–CS is catalysis. Green nanocomposite based on GO–CS have demonstrated high thermal stability (165°C) in differential scanning calorimetry (DSC) in comparison with pure CS (118–119°C), both were used as a support for novel catalyst. In this research, average size distribution of 50 nm was measured by atomic force microscopy (AFM) for GO–CS nanocomposite synthesized in free-solvent conditions. Efficient synthesis of 2,4,5-trisubstituied-1H-imidazoles were done, GO–CS in catalytic amount was combined with benzyl 2 or benzoin 1, benzaldehyde 3 and ammonium acetate at 120°C that shows great thermal stability of GO–CS system [102]. Another novel catalyst was developed for reduction of aromatic nitroarenes and azo dye degradation [103]. Silver (AgNPs) and gold (AuNPs) nanoparticles were attached onto GO–CS system in order to avoid aggregations of either Ag or Au nanoparticles which affect its catalytic activity. Both GO–CS-AgNPs and GO–CS-AuNPs catalysts were obtained in similar process using 0.1 M solution of silver nitrate ($AgNO_3$) and tetrachloroauric (III) acid hydrate respectively in a solution of sodium borohydride ($NaBH_4$). Particles of 20 nm for AgNPs and 5 nm for AuNPs were observed by high resolution trans-

mission electron microscopy (HR-TEM) that demonstrates homogeneous deposition of particles. The excellent catalytic activity and selective reduction of nitroarenes was mainly attributed to the high surface area of GO–CS system which improves adsorption of organic substrates, and to the presence of $–NH_2$ and –OH groups in GO–CS system which might assist the stabilization and attraction of particles toward the catalytic sites, because of the combination of hydrophobic–hydrophilic nature present in GO and CS.

4.3.1.1. Covalent attachment of chitosan onto GO through a $KMnO_4$ redox system

Functionalization of GO with CS by redox system with $KMnO_4$, H_2SO_4, and malic acid also has been reported [75]. In this approach, covalent attachment of CS onto GO was done varying temperature conditions, this shows influence over morphology and features of the final material produced. A better dispersion behavior was obtained as a result of chemical modification (grafting) originated from the interaction of GO and CS functional groups. As can be seen in **Figure 8a**, well-exfoliated graphene oxide sheet alike a thin film and wrinkled surface is shown. Additionally, TEM images of CS grafted on GO exhibit the differences on morphology acquired in different conditions **Figure 8b–d**. At the lowest temperature, GO sheet is completely covered by CS. However, as the temperature is increase (75–80°C), CS only partially covers the GO sheets, and finally for the highest temperature, the GO–CS system shows great differences in its morphology, like a scrolled material. This can be attributable to the loss of free water in CS that increases as the temperature does, impacting on the amount of water and hydrogen bonds formed during grafting. Dispersion behavior of different GO–CS produced on water and hexane. A water stable dispersion even 24 h after the sonication process was

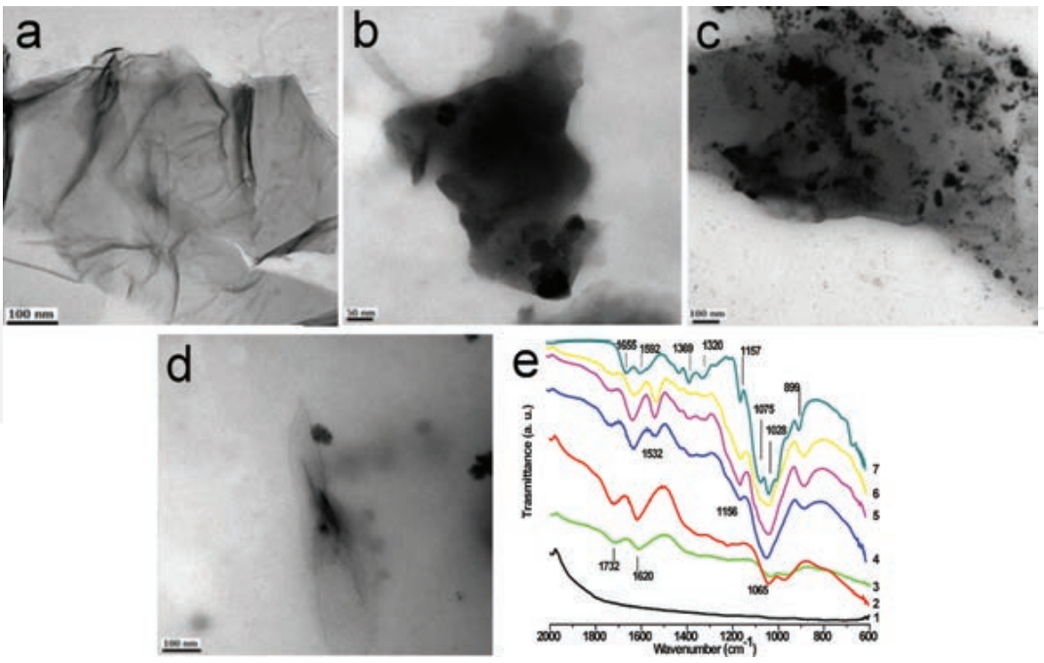


Figure 8. TEM images of (a) GO; (b) GO–CS obtained at 55–60°C; (c) GO–CS obtained at 75–80°C; (d) GO–CS obtained at 95–100°C; (e) FTIR spectra of (1) graphite; (2) graphite oxide; (3)GO; (4) GO–CS obtained at 55–60°C; (5) GO–CS obtained at 75–80°C; (6) GO–CS obtained at 95–100°C and (7) CS.

http://dx.doi.org/10.5772/64001

observed, unlike in hexane non-polar solvent which shows poor dispersion and rapid precipitation of GO–CS. In addition, AFM measurements show a roughness between 3 and 6 nm for the GO–CS which is the result of bundles of CS chains grafted on GO that can be observed as dark dense zones in TEM images.

FTIR analysis was done in order to provide evidence about the chemical modification of graphite, and grafting of CS onto GO. The appearance of new signals respecting the interaction of moieties presents in both GO and CS can be clearly seen in the **Figure 8e**. Signal from new amides or carbamate esters formed during grafting, this band appears in 1535 cm^{-1} attributed to the combination of ν(C–N) and δ(CNH). Both, the band at 1156 cm^{-1} corresponding to ν_a(C–O–C) and signal at 899 cm^{-1} for C–O–C were detected, they are related with glycosidic linkage. The latter are typical in chitosan, whereas after grafting they are shifted to 881 cm^{-1} in GO–CS systems that show the modifications of C–O–C bond vibrations and the interaction of GO–CS hybrids. In addition, Raman spectroscopy and energy dispersive X-ray spectroscopy (EDS) characterization techniques were used in order to corroborate the grafting of CS onto GO.

Finally based on previous works [99, 100] and evidence obtained in FTIR measurements, few reactions can be proposed for the novel bonds as a result of grafting of CS. As can be seen in Eqs. (3)–(5), first, linkage can be done by carbonyl moieties ((3) and (4)) and second with breaking of epoxy groups (5). Despite that other reactions can be carried out but evidence provided by FTIR points out just the aforementioned.

$$GO-COOH+CS-NH_2 \xrightarrow[H^+,\ malic\ ac.\ \square]{KMnO_4} GO-CONH-CS+Subproduct \tag{3}$$

$$GO-COOH+CS-OH \xrightarrow[H^+,\ malic\ ac.\ \square]{KMnO_4} GO-COO-CS+Subproducts \tag{4}$$

Subproducts = HO, RH, ROH (R = Radical from malic acid)



(5)

4.3.2. Non-covalent functionalization of GO and rGO with CS

Non-covalent functionalization of GO and rGO has been done through different ways such as hydrogen bonding, electrostatic interactions, Van der Waals forces, and ionic interactions. Electrostatic forces in functionalized GO have been reported in order to develop applications

such as hemolytic activity and nanocomposites [104–107]. Li et al. reported removal of single or multi-system ions based on Cu (II), Pb (II) and Cd (II). GO was functionalized with a sulfhydryl compound and CS resulting in CS–GO–SH adsorbent material, basically due to the affinity of CS, known as a cationic polymer with plenty –OH and $–NH_2$ groups and negative charged in GO–SH complexes. In this work, ultrasonication was applied to yield GO–CS–SH nanocomposite; sulfhydryl groups were previously grafted on GO reacting in stirring with 4-aminothiophenol. Adsorption tests result in Q_{max} of 235, 226, and 117 mg/g for Cu (II), Pb (II), and Cd (II), respectively, from a starting concentration of 250 mg/L, and thus, a higher adsorption was obtained in comparison with other results reported with GO and CS as adsorbent. This suggests a synergistic effect originated by increasing the specific surface area and space between CS and GO–SH. Moreover, operational factors such as pH, adsorbent dosage, and temperature play important roles in results [107]. Other approach about electrostatic interactions to functionalize GO was reported by Liao et al., they discussed the effect of GO size and coated GO over hemolytic activity. GO obtained in different exfoliation parameters were tested by methylthiazolyldiphenyl-tetrazolium bromide (MTT) and water-soluble tetrazolium salt (ST-8) to show blood compatibility. The functionalization of GO with CS reveals lower hemolytic activity in comparison of GO sheets; this can be attributable to disruption of red blood cells membrane (RBC) as a result of the strong electrostatic interaction between oxygenated functional groups of GO sheets with negative charge and positively charged phosphatidylcholine lipids of RBC outer membrane [104]. Unlike a traditional CS polymer with $–NH_2$ groups which only become charged in acidic media, quaternized CS (QCS) is a polymer attached with quaternary ammonium groups which confers a cationic polyelectrolyte permanently charged feature [108]. Consequently, cellulosic paper fibers can be cover with a positively charged coating made of QCS which attract the negatively charged GO sheets. So QCS can be used as a "glue" linking cellulose fibers to GO via electrostatic interactions. This was reported by Ling and co-workers in order to fabricate composite paper in addition to load GO with AuNPs and its subsequent reduction by hydrogen iodide vapor. The final material shows an outstanding conductivity of 831 S/m [105]. Another interesting applications recently reported are Janus GO–CS membrane; in this work; non-covalently assembly GO–CS membrane was used as a support of poly(styrene) (PS) and poly (N,N-dimethyl methacrylate) (PDMAEMA) in upper and lower membrane surface; respectively. Photografting and photopolymerization were used to yield Janus membranes a possible material for applications such as sensing or catalyst as a result of its versatility [109].

On the other hand, another route of non-covalent functionalization of GO is through hydrogen bonding which has been reported to develop novel nanocomposites. Recently; a facile GO/CS conducting biocompatible hydrogel production method by extrusion printing was reported. CS and lactic acid (LA) as matrix and GO as reinforcement material were used, and L929 cells were cultured in diluted GO–CS–LA dispersions and were compared with GO–CS–LA nanocomposites.

Another via of non-covalent functionalization of GO is the formation of hydrogen bond with CS which has been reported to develop novel nanocomposites. As a result of homogeneous distribution as well as excellent mechanical properties achieved in GO–CS nanocomposites

originated from non-covalent interactions, high-performance nanocomposites have been prepared [110]. High mechanical properties exhibited in GO–CS nanocomposite can be used for drug delivery, GO–CS nanocomposites offer a platform to yield a tunable control through pH transdermal system for drug release [111]. Recently, another approach was done using CS and lactic acid (LA) as matrix and GO as reinforcement material by extrusion printing. Due to the relevance of the morphology, dimensions, shape, and biocompatibility in materials for tissue engineering, GO–CS was used to yield conducting biocompatible hydrogel. FTIR shows strong interaction by hydrogen bond between GO–CS–LA. Additionally L929 cells were cultured in composites; first diluted GO–CS–LA dispersions were used to note cell growth. Cell growth showed an increment of cell density 10–15 times ($45 \pm 4E^4$ cells cm^{-2} and 1.5% dead cells) in comparison to the original amount. No cell showed inclusion of dark material in either cytoplasm or any organelle; this was observed by bright field microscope. Second for GO–CS–LA films and scaffolds; no toxicity or changes on migration were observed in cells; moreover, mechanical properties were enhanced by the addition of GO having increments in tensile strength of 320% and 162% for dry and wet state for GO–CS–LA nanocomposite with only 3 wt% of GO added [112].

Due to the versatility and interesting capacity of self-healing against damage, polymeric gels have attracted great attention. GO and CS hydrogels were prepared by non-covalent interactions; in this regard, GO can be considered as a 2D cross-linker as a result of functional groups present in both faces of GO sheets. Electrostatic and hydrogen bond are the predominant interaction in this kind of materials according with the report [113]. Water, CS, and GO are the molecules present in hydrogel, interacting mainly by electrostatic forces when mixed at room temperature. Particularly CS shows a compact state owing to hydrogen bond present in its structure, thus restricting the interaction with GO, this is diminished with the increase of temperature of hydrogel preparation according with the methodology. This kind of materials can be applied in fields such as biomaterials, absorbents, and so on. For example, recently heparin/GO–CS hybrid hydrogel (Hep-GO–CS) were synthetized for bilirubin adsorption. Adsorption measurements in phosphate buffer solution (PBS) show for Hep-GO–CS four times adsorption capacity than CS hydrogel; this can be attributable to GO added to hydrogel. Additionally, this material exhibits good hemocompatibility and low degree of hemolysis in the tests realized [114]. On the other hand, other applications for GO–CS system based on both electrostatic interactions and hydrogen bond have been reported in fields such as nanocomposites for electrochemical biosensors [115], pathogen agent detection [116], membranes in microbial fuel cells [117], and cell growth [118]. Additionally, preparation of poly(vinyl alcohol) PVA–CS nanocomposite reinforced by rGO was reported; simultaneously, reduction and functionalization were done and synergistic effect by the interaction of rGO–CS–PVA was demonstrated with high-performance nanocomposite obtained. CS acts as a bridge between rGO and PVA enhancing the quantity of formed hydrogen bonds, which improved mechanical properties taking for instance an increase of 40% in value of tensile strength in comparison of CS–PVA polymer [119].

As can be seen in **Figure 9**, multifunctional rGO magnetic nanosheet functionalized via non-covalent with chitosan (rGOMCS) was developed for *Pseudomonas aeruginosa* (BCRC 10303)

and *Staphylococcus aureus* (BCRC 1045) detection in aqueous suspension and mouse blood. Owing to its inherent fluorescence properties and high surface area, rGO as a support to magnetic nanoparticles enhanced detection of bacteria in fluorescence spectroscopy and matrix-assisted laser desorption/ionization mass spectrometry (MALDI-MS). On one hand, fluorescence as bacteria detection method has been used widely, in spite of interference created by biomolecules in biological samples, furthermore external factors, among others make it a complicated task. On the other hand, great influence of CS and complementary effect of functional groups on graphene attached on rGOMCS was observed over bacteria in MALDI-MS. This allowed different non-covalent interactions (hydrogen bond, hydrophobic and electrostatic interactions, acid-base interactions, π–π interactions and polar functional groups interactions) together with pathogen agents reflecting high adsorption. Additionally, Abdelhamid et al. [116] reported thermodynamic analysis which reveals better affinity of CS to BCRC 1045 as a result of increment on peptidoglycan content and consequently better sensitivity for this pathogen agent.

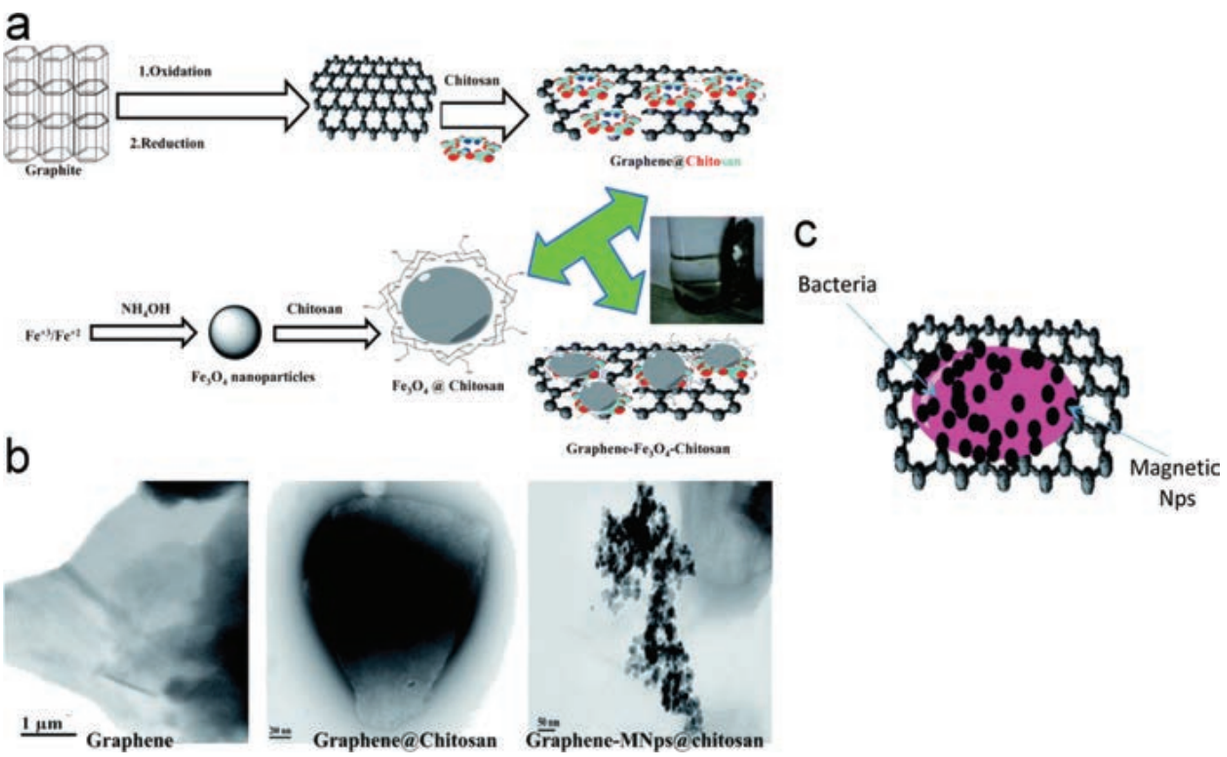


Figure 9. (a) Schematic diagram of the assembly of rGOMCS; (b) TEM images of rGO functionalized with magnetic particles and CS (c) Interaction between bacteria and rGOMCS. (Adapted from [116] with permission of The Royal Society of Chemistry).

ζ potential measurements reveal the influence of ionic interactions between rGO–CS solutions, another via of non-covalent functionalization of rGO. First, notable differences in the responses of GO–CS solutions were observed only changing the order of aggregation of the components.

http://dx.doi.org/10.5772/64001

In the **Figure 10**, as can be seen when GO is added to CS solution the GO sheets are wrapped rapidly by ionic interactions with considerable amount of CS (ζ potential of +40 mV); however, if the GO is added greatly dispersed in solution to CS forms a "bridging" flocculation as a result of attachment of two or more GO sheets to polymer chain (ζ potential of +8 mV). Second, one can take advantage that after GO reduction by L-AA in the presence of CS was done; the remaining functional groups on rGO and $–NH_2$ groups in CS are still available for non-covalent functionalization. This offers the possibility to control and change behavior of rGO–CS solutions inasmuch as pH is changed. ζ potential measurements show both behaviors on pH 6 (+33 mV) and at pH 7 (-9 mV) for a stable suspension and formation of agglomerates, respectively. It can be explained because at low pH, $–NH_2$ groups are protonated creating a good environment for electrostatic repulsion between rGO sheets. In spite of that, if the pH is increased the intermolecular repulsion tend to decrease, originated by the deprotonation of NH_2 groups of CS [60]. Ko et al., performed a nanocomposite for growth of *Escherichia coli* bacteria. They carried out the simultaneous reduction and non-covalent functionalization of GO in acid media solutions, attributing to remaining protonated $–NH_3^+$ groups on CS the contributions for the well-dispersed rGO–CS system. Moreover, enhanced antibacterial activity for *E. coli* was detected [120]. In **Table 2** are summarized some applications for both GO-CS and rGO-CS with covalent and non-covalent interactions.

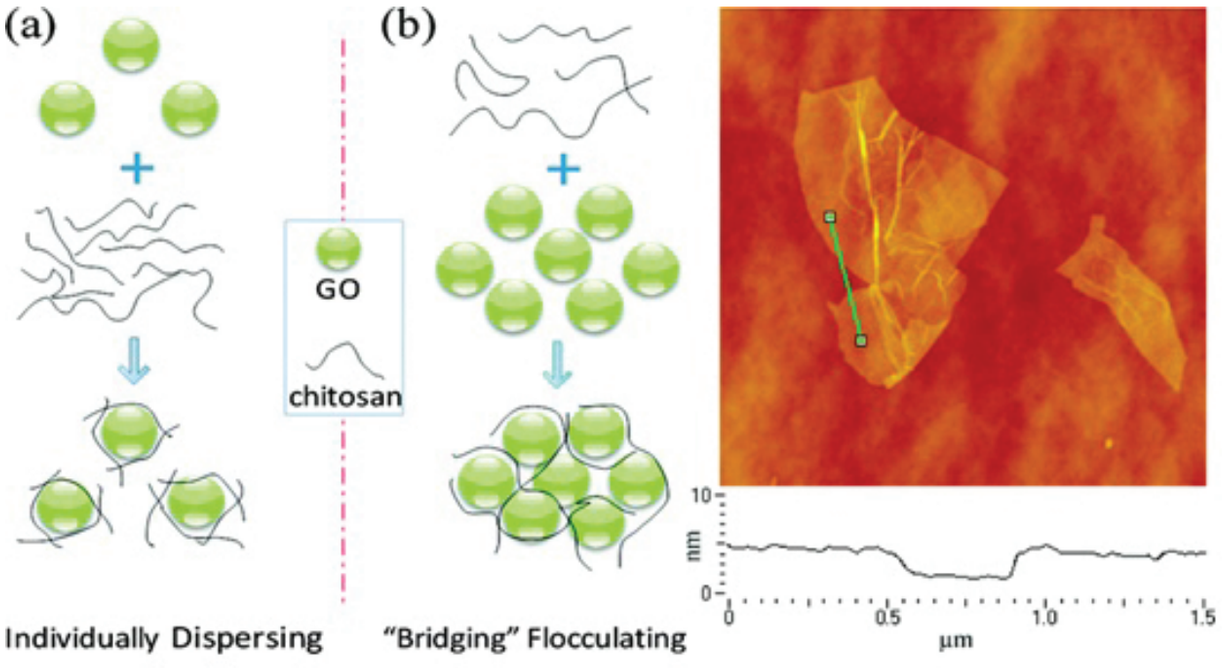


Figure 10. (a) Schematic diagram of GO–CS suspensions behavior as a result of the variation in the order of the addition of components. (b) Measurements taken by atomic force microscopy (AFM) of rGO extracted from rGO–CS suspension and deposited in cleaved mica. (Adapted with permission from [60]. Copyright 2016 American Chemical Society).

Potential application	**Interaction GO–CS or r GO–CS *via covalent***	**Reference**
Water treatment (U(vi) removal)	Amidation	[101]
Water treatment (antifouling)	Amidation	[100]
Water treatment (removal Cr(IV))	Amidation	[97]
Water treatment (desalting)	Nucleophilic addition (Ring opening)	[87]
Water treatment (Fuschine removal)	Amidation	[99]
DNA biosensor	Amidation	[88]
Drug delivery	Amidation	[89]
Drug delivery	Amidation	[90]
Lipase immobilization	Amidation	[92]
Osteoblasts growth	Amidation	[91]
Growth of cells C3H10T1/2	Amidation	[93]
Drug delivery (Fluorescein sodium)	Amidation	[94]
Nanocatalyst	Amidation	[103]
Nanocatalyst	Amidation	[102]
Nanocomposite (GO–CS –HAP, bioactivity)	Amidation	[96]
Nanocomposite	Amidation	[84]
Nanocomposite	Amidation	[121]
Nanocomposite	Amidation/Esterification	[21]
Nanocomposite	Nucleophilic addition (Ring opening)	[86]
Nanocomposite	Esterification	[85]
Potential application	Interaction GO–CS or r GO–CS *via non-covalent*	
Hemolytic activity	Electrostatic adsorption	[104]
Multifunctional paper	Electrostatic interaction	[105]
Glucose and urea detection	Electrostatic interaction	[106]
Removal contaminants	Electrostatic interaction	[107]
Nanocomposite (PVA)	Hydrogen bond/electrostatic interaction	[119]
Supramolecular hydrogel	Hydrogen bond/electrostatic interaction	[113]
L929 cells and MG-63 cells growth	Hydrogen bond/electrostatic interaction	[118]
Bulirubin adsorbent hydrogel	Hydrogen bond/electrostatic interaction	[114]
Electrochemical electrode	Hydrogen bond/electrostatic interaction	[115]
E. Coli growth	Hydrogen bond/electrostatic interaction	[117]
Sensor of *Pseudomonas aeruginosa and Staphylococcus aureus*	Hydrogen bond/electrostatic attractions	[116]

Potential application	Interaction GO–CS or r GO–CS *via covalent*	Reference
Nanocomposite	Hydrogen bond/electrostatic attractions	[122]
Janus membranes	Polycationic interaction	[109]
pH responsive nanocomposite	GO-Ionic interactions (Electrostatic)	[60]
pH responsive nanocomposite	rGO ionic interaction/hydrogen bond	[60]
Nanocomposite	Hydrogen bond	[110]
Fluorescein sodium	Hydrogen bond	[111]
L929 cells growth	Hydrogen bond	[112]
Antibacterial activity	Van der Walls/Ionic/hydrogen bonding	[120]

Table 2. Functionalization of GO and rGO by CS and its progress in different fields of application.

5. Conclusions

During the last years, many efforts have been done in order to exploit the outstanding properties of graphenic materials in fields such as catalysis, nanocomposites, cell batteries, and so on. As a result of its versatility, the chemically route to produce graphene oxide and reduced graphene oxide offers a possible solution for requirements about scalability, cost-effective, and easy way to obtain suited amounts of graphene for its applicability. Both GO and rGO can take some advantages over pristine graphene because of the rich chemistry of their functional groups present on the surface. These groups can be used as points to anchor specific molecules according the necessities, which granted the shown multifunctionality. Specifically, in rGO, the restoration of sp^2 domains through the reduction reaction offers a conductive material which can be applied in fields where the conductivity is overriding. Additionally, emerging routes to achieve non-covalent and covalent functionalization of graphenic materials have been reported. In this chapter, we outline recent progress in covalent and non-covalent functionalization of graphenic materials with biopolymers such as keratin and chitosan. Both are aimed on the development of a multifunctional platform capable of being used in different fields.

Functionalization of graphene-based materials with biomolecules offers an additional advantage to orient these materials for biological applications, increasing, for example, their compatibility. Biofunctionalization with small or medium size biopolymer chains, as in the case of some proteins or polysaccharides, enables the formation of hybrid or conjugated systems through a series of several interaction or reaction points. This, as a result of the presence of different chemical functionalities, as in the case of keratin, or a repeated functional group, as in the case of chitosan, in each polymeric unit. This aspect allows to fully cover the nanocarbon surface with along with a strong biomolecule immobilization.

To the best of our knowledge, as we have discussed in this chapter, there are just a couple of works related to the functionalization of graphenic materials through a redox reaction system. This approach has been commonly used to achieve high degree of attachments in natural and

synthetic polymeric materials. A redox reaction brings the benefit to yield a random covalent functionalization practically using all the available chemical groups in both materials, at relatively low reaction temperature. Therefore, the resulting surface will possess few functional groups, if any at all. In the case of the non-covalent functionalization of reduced graphene oxide, the opposite behavior will take place. The functional groups of the biomolecule will be exposed on the conjugated system surface. This proves its utility if an additional functionalization, specific group reactions, or a further adsorption process is desired.

We want to awake the interest of the reader in the study of these approaches and to compare their advantages in disadvantages for other systems.

Author details

Edgar Jimenez-Cervantes Amieva[1,2], Juventino López-Barroso[1],
Ana Laura Martínez-Hernández[1*] and Carlos Velasco-Santos[1]

*Address all correspondence to: almh72@gmail.com

1 Division of Postgraduate Studies and Research, Technological Institute of Queretaro, Santiago de Querétaro, Querétaro, Mexico

2 Centre of Applied Physics and Advanced Technology, National Autonomous University of Mexico, Campus Juriquilla, Querétaro, Mexico

References

[1] Das S., Choi W. Graphene synthesis. In: Choi W., Lee J.W., editors. Graphene: synthesis and applications. Boca Raton, FL: CRC Press, Taylor and Francis group; 2012. p. 27–63.

[2] Novoselov K.S., Geim A.K., Morozov S.V., Jiang D., Zhang Y., Dubonos S.V., Grigorieva I.V., Firsov A.A. Electric field effect in atomically thin carbon films. Science. 2004;306(5696):666–669. doi:10.1126/science.1102896

[3] Sundaram R.S. Chemically derived graphene. In: Skákalová V., Schäffel F., Bachmatiuk A., Rümmeli M.H., editors. Graphene: properties, preparation, characterisation and devices. Sawston, Cambridge: Woodhead Publishing; 2014. p. 50–80. doi: 10.1533/9780857099334.1.50

[4] Ibrahim I., Rümmeli M.H. Mechanical exfoliation. In: Warner J.H., Schäffel F., Bachmatiuk A., Rümmeli M.H., editors. Graphene: fundamentals and emergent applications. Kidlington, Oxford: Elsevier; 2013. p. 129–137. doi:10.1016/B978-0-12-394593-8.00004-7

[5] Zhong Y.L., Tian Z., Simon G.P., Li D. Scalable production of graphene via wet chemistry: progress and challenges. Materials Today. 2015;18(2):73–78. doi:10.1016/j.mattod.2014.08.019

[6] Hummers W., Offeman R.E. Preparation of graphitic oxide. Journal of the American Chemical Society. 1958;80(6):1339. doi:10.1021/ja01539a017

[7] Bonaccorso F., Lombardo A., Hasan T., Sun Z., Colombo L., Ferrari A.C. Production and processing of graphene and 2d crystals. Materials Today. 2012;15(12):564–589. doi:10.1016/S1369-7021(13)70014-2

[8] Chen G., Weng W., Wu D., Wu C., Lu J., Wang P., Chen X. Preparation and characterization of graphite nanosheets from ultrasonic powdering technique. Carbon. 2004;42(4):753–759. doi:10.1016/j.carbon.2003.12.074

[9] Warner J.H. Reduced graphene oxide. In: Warner J.H., Schäffel F., Bachmatiuk A., Rümmeli M.H., editors. Graphene: fundamentals and emergent applications. Kidlington, Oxford: Elsevier; 2013. p. 155–162. doi:10.1016/B978-0-12-394593-8.00004-7

[10] Pei S., Cheng H.-M. The reduction of graphene oxide. Carbon. 2012;50(9):3210–3228. doi:10.1016/j.carbon.2011.11.010

[11] Hu K., Kulkarni D.D., Choi I., Tsukruk V.V. Graphene-polymer nanocomposites for structural and functional applications. Progress in Polymer Science. 2014;39(11):1934–1972. doi:10.1016/j.progpolymsci.2014.03.001

[12] Loh K.P., Bao Q., Eda G., Chhowalla M. Graphene oxide as a chemically tunable platform for optical applications. Nature Chemistry. 2010;2(12):1015–1024. doi:10.1038/nchem.907

[13] Lerf A., He H., Forster M., Klinowski J. Structure of graphite oxide revisited. The Journal of Physical Chemistry B. 1998;102(23):4477–4482. doi:10.1021/jp9731821

[14] Gao W., Alemany L.B., Ci L., Ajayan P.M. New insights into the structure and reduction of graphite oxide. Nature Chemistry. 2009;1(5):403–408. doi:10.1038/nchem.281

[15] Li D., Mueller M.B., Gilje S., Kaner R.B., Wallace G.G. Processable aqueous dispersions of graphene nanosheets. Nature Nanotechnology. 2008;3(2):101–105. doi:10.1038/nnano.2007.451

[16] Dreyer D.R., Park S., Bielawski C.W., Ruoff R.S. The chemistry of graphene oxide. Chemical Society Reviews. 2010;39(1):228–240. doi:10.1039/B917103G

[17] Hernandez Y., Pang S., Feng X., Müllen K. Graphene and its synthesis. In: Matyjaszewski K., Möller M., editors. Polymer science: a comprehensive reference. Amsterdam, NL: Elsevier; 2012. p. 415–438. doi:10.1016/B978-0-444-53349-4.00216-8

[18] Inagaki M., Kang F., Toyoda M., Konno H. Advanced materials science and engineering of carbon. Beijing, China: Elsevier & Tsinghua Univ. Press; 2013. 434 p. doi:10.1016/B978-0-12-407789-8.00003-X

[19] Whitener K.E., Sheehan P.E. Graphene synthesis. Diamond and Related Materials. 2014;46:25–34. doi:10.1016/j.diamond.2014.04.006

[20] Stankovich S., Dikin D.A., Piner R.D., Kohlhaas K.A., Kleinhammes A., Jia Y., et al. Synthesis of graphene-based nanosheets via chemical reduction of exfoliated graphite oxide. Carbon. 2007;45:1558–1565. doi:10.1016/j.carbon.2007.02.034

[21] Bustos-Ramírez K., Martínez-Hernández A.L., Martínez-Barrera G., Icaza M.D., Castaño V.M., Velasco-Santos C. Covalently bonded chitosan on graphene oxide via redox reaction. Materials. 2013;6(3):911-926. doi:10.3390/ma6030911

[22] Kim J., Cote L.J., Kim F., Yuan W., Shull K.R., Huang, J. Graphene oxide sheets at interfaces. Journal of the American Chemical Society. 2010;132(23):8180–8186. doi: 10.1021/ja102777p

[23] Whitby R.L.D. Chemical control of graphene architecture: tailoring shape and properties. ACS Nano. 2014;8(10):9733–9754. doi:10.1021/nn504544h

[24] Hu Y., Song S., Lopez-Valdivieso A. Effects of oxidation on the defect of reduced graphene oxides in graphene preparation. Journal of Colloid and Interface Science. 2015;450:68–73. doi:10.1016/j.jcis.2015.02.059

[25] Zhao J., Pei S., Ren W., Gao L., Cheng H.-M. Efficient preparation of large-area graphene oxide sheets for transparent conductive films. ACS Nano. 2010;4(9):5245–5252. doi: 10.1021/nn1015506

[26] Chua C.K., Pumera M. Chemical reduction of graphene oxide: a synthetic chemistry viewpoint. Chemical Society Reviews. 2014;43(1):291–312. doi:10.1039/C3CS60303B

[27] Liang Y., Frisch J., Zhi L., Norouzi-Arasi H., Feng X., Rabe J.P., et al. Transparent, highly conductive graphene electrodes from acetylene-assisted thermolysis of graphite oxide sheets and nanographene molecules. Nanotechnology. 2009;20(43):434007. doi: 10.1088/0957-4484/20/43/434007

[28] Su Q., Pang S., Alijani V., Li C., Feng X., Müllen K. Composites of graphene with large aromatic molecules. Advanced Materials. 2009;21(31):3191–3195. doi:10.1002/adma. 200803808

[29] Schniepp H.C., Li J.-L., McAllister M.J., Sai H., Herrera-Alonso M., Adamson D.H., et al. Functionalized single graphene sheets derived from splitting graphite oxide. The Journal of Physical Chemistry B. 2006;110(17):8535–8539. doi:10.1021/jp060936f

[30] Wu Z.-S., Ren W., Gao L., Zhao J., Chen Z., Liu B., et al. Synthesis of graphene sheets with high electrical conductivity and good thermal stability by hydrogen arc discharge exfoliation. ACS Nano. 2009;3(2):411–417. doi:10.1021/nn900020u

[31] McAllister M.J., Li J.-L., Adamson D.H., Schniepp H.C., Abdala A.A., Liu J., et al. Single sheet functionalized graphene by oxidation and thermal expansion of graphite. Chemistry of Materials. 2007;19(18):4396–4404. doi:10.1021/cm0630800

[32] Toh S.Y., Loh K.S., Kamarudin S.K., Daud W.R.W. Graphene production via electrochemical reduction of graphene oxide: synthesis and characterisation. Chemical Engineering Journal. 2014;251:422–434. doi:10.1016/j.cej.2014.04.004

[33] Guo H.-L., Wang X.-F., Qian Q.-Y., Wang F.-B., Xia, X.-H. A green approach to the synthesis of graphene nanosheets. ACS Nano. 2009;3(9):2653–2659. doi:10.1021/nn900227d

[34] Gao J., Liu F., Liu Y., Ma N., Wang Z., Zhang X. Environment-friendly method to produce graphene that employs vitamin C and amino acid. Chemistry of Materials. 2010;22(7):2213–2218. doi:10.1021/cm902635j

[35] Zhang J., Yang H., Shen G., Cheng P., Zhang J., Guo S. Reduction of graphene oxide via L-ascorbic acid. Chemical Communications. 2010;46(7):1112–1114. doi:10.1039/B917705A

[36] Tabrizi M.A., Varkani J.N. Green synthesis of reduced graphene oxide decorated with gold nanoparticles and its glucose sensing application. Sensors and Actuators B: Chemical. 2014;202:475–482. doi:10.1016/j.snb.2014.05.099

[37] Suresh D., Nagabhushana H., Sharma S.C. Clove extract mediated facile green reduction of graphene oxide, its dye elimination and antioxidant properties. Materials Letters. 2015;142:4–6. doi:10.1016/j.matlet.2014.11.073

[38] Suresh D., Nethravathi P.C., Nagabhushana H., Sharma S.C. Spinach assisted green reduction of graphene oxide and its antioxidant and dye absorption properties. Ceramics International. 2015;41(3):4810–4813. doi:10.1016/j.ceramint.2014.12.036

[39] Suresh D., Kumar M.P., Nagabhushana H., Sharma S.C. Cinnamon supported facile green reduction of graphene oxide, its dye elimination and antioxidant activities. Materials Letters. 2015;151:93–95. doi:10.1016/j.matlet.2015.03.035

[40] Akhavan O., Ghaderi E., Abouei E., Hatamie S., Ghasemi E.. Accelerated differentiation of neural stem cells into neurons on ginseng-reduced graphene oxide sheets. Carbon. 2014;66:395–406. doi:10.1016/j.carbon.2013.09.015

[41] He D., Peng Z., Gong W., Luo Y., Zhao P., Kong L. Mechanism of a green graphene oxide reduction with reusable potassium carbonate. RSC Advances. 2015;5(16):11966–11972. doi:10.1039/C4RA14511A

[42] Akhavan O., Azimirad R., Gholizadeh H.T., Ghorbani F.. Hydrogen-rich water for green reduction of graphene oxide suspensions. International Journal of Hydrogen Energy. 2015;40(16):5553–5560. doi:10.1016/j.ijhydene.2015.02.106

[43] Georgakilas V., Otyepka M., Bourlinos A.B., Chandra V., Kim N., Kemp K.C., et al. Functionalization of graphene: covalent and non-covalent approaches, derivatives and applications. Chemical Reviews. 2012;112(11):6156–6214. doi:10.1021/cr3000412

[44] Hirsch, A. The era of carbon allotropes. Nature Materials. 2010;9(11):868–871. doi: 10.1038/nmat2885

[45] Georgakilas V. Covalent attachment of organic functional groups on pristine graphene. In: Georgakilas V., editor. Functionalization of graphene. Weinheim, Germany: Wiley-VCH; 2014. p. 21–58.

[46] Spinato C., Ménard-Moyon C., Bianco A. Chemical functionalization of graphene for biomedical applications. In: Georgakilas V., editor. Functionalization of graphene. Weinheim, Germany: Wiley-VCH; 2014. p. 95–138.

[47] Ju H., Zhang X., Wang J. NanoBiosensing: principles, development and application. New York, NY: Springer Science & Business Media; 2011. 586 p. doi:10.1007/978-1-4419-9622-0

[48] Georgakilas V. Addition of organic groups through reactions with oxygen species of graphene oxide. In: Georgakilas V., editor. Functionalization of graphene. Weinheim, Germany: Wiley-VCH; 2014. p. 59–94.

[49] Luong N.D., Sinh L.H., Johansson L.-S., Campell J., Seppälä J. Functional graphene by thiol-ene click chemistry. Chemistry–A European Journal. 2015;21(8):3183–3186. doi: 10.1002/chem.201405734

[50] Ferrari A.C., Bonaccorso F., Fal'Ko V., Novoselov K.S., Roche S., Bøggild P., et al. Science and technology roadmap for graphene, related two-dimensional crystals, and hybrid systems. Nanoscale. 2015;7(11):4598–4810. doi:10.1039/C4NR01600A

[51] Kemp K.C., Cho Y., Chandra V., Kim K.S. Noncovalent functionalization of graphene. In: Georgakilas V., editor. Functionalization of graphene. Weinheim, Germany: Wiley-VCH; 2014. p. 199–218.

[52] Pavlidis I.V., Patila M., Polydera A.C., Gournis D., Stamatis H. Immobilization of enzymes and other biomolecules on graphene. In: Georgakilas V., editor. Functionalization of graphene. Weinheim, Germany: Wiley-VCH; 2014. p. 139–172.

[53] Moench I., Meye A., Leonhardt A. Ferromagnetic filled carbon nanotubes as novel and potential containers for anticancer treatment strategies. In: Kumar C.S.S.R., editor. Series: nanotechnologies for the life sciences vol. 6: nanomaterials for cancer therapy. Weinheim, Germany: Wiley-VCH; 2007. p. 259–337. doi: 10.1002/9783527610419.ntls0068

[54] Georgakilas V. Functionalization of graphene by other carbon nanostructures. In: Georgakilas V., editor. Functionalization of graphene. Weinheim, Germany: Wiley-VCH; 2014. p. 255–282.

[55] Zhang M., Yin B.-C., Wang X.-F., Ye B.-C. Interaction of peptides with graphene oxide and its application for real-time monitoring of protease activity. Chemical Communications. 2011;47(8):2399–2401. doi:10.1039/C0CC04887A

[56] Lu F., Zhang S., Gao H., Jia H., Zheng L. Protein-decorated reduced oxide graphene composite and its application to SERS. ACS Applied Materials & Interfaces. 2012;4(6): 3278–3284. doi:10.1021/am300634n

[57] Zeng Q., Cheng J., Tang L., Liu X., Liu Y., Li J., et al. Self-assembled graphene–enzyme hierarchical nanostructures for electrochemical biosensing. Advanced Functional Materials. 2010;20(19):3366–3372. doi:10.1002/adfm.201000540

[58] Liu J., Li Y., Li Y., Li J., Deng Z. Noncovalent DNA decorations of graphene oxide and reduced graphene oxide toward water-soluble metal–carbon hybrid nanostructures via self-assembly. Journal of Materials Chemistry. 2010;20(5):900–906. doi:10.1039/B917752C

[59] Liu S.-J., Wen Q., Tang L.-J., Jiang J.-H. Phospholipid–graphene nanoassembly as a fluorescence biosensor for sensitive detection of phospholipase D activity. Analytical Chemistry. 2012;84(14):5944–5950. doi:10.1021/ac300539s

[60] Fang M., Long J., Zhao W., Wang L., Chen G. pH-responsive chitosan-mediated graphene dispersions. Langmuir. 2010;26(22):16771–16774. doi:10.1021/la102703b

[61] Kouloumpis A., Zygouri P., Dimos K., Gournis D. Layer-by-layer assembly of graphene-based hybrid materials. In: Georgakilas V., editor. Functionalization of graphene. Weinheim, Germany: Wiley-VCH; 2014. p. 359–399.

[62] Yang K., Feng L., Shi X., Liu Z. Nano-graphene in biomedicine: theranostic applications. Chemical Society Reviews. 2013;42(2):530–547. doi:10.1039/C2CS35342C

[63] Wang Y., Li Z., Wang J., Li J., Lin Y. Graphene and graphene oxide: biofunctionalization and applications in biotechnology. Trends in biotechnology. 2011;29(5):205–212. doi: 10.1016/j.tibtech.2011.01.008

[64] Nyanhongo G.S., Steiner W., Gübitz G.M., editors. Biofunctionalization of polymers and their applications. Berlin Heidelberg: Springer-Verlag; 2011. 288 p. doi:10.1007/978-3-642-21949-8

[65] Wikimedia Foundation. Biofunctionalisation [Internet]. February 8 2015. Available from: http://en.wikipedia.org/wiki/Biofunctionalisation [Accessed: May 7 2015]

[66] Rodríguez-González C., Martínez-Hernández A.L., Castan~o V.M., Kharissova O.V., Ruoff R.S., Velasco-Santos C. Polysaccharide nanocomposites reinforced with graphene oxide and keratin-grafted graphene oxide. Industrial & Engineering Chemistry Research. 2012;51(9):3619–3629. doi:10.1021/ie200742x

[67] Amieva E.J.C., Fuentes-Ramirez R., Martinez-Hernandez A.L., Millan-Chiu B., Lopez-Marin L.M., Castaño V.M., et al. Graphene oxide and reduced graphene oxide modification with polypeptide chains from chicken feather keratin. Journal of Alloys and Compounds. 2015;643:S137–S143. doi:10.1016/j.jallcom.2014.12.062

[68] Schrooyen P.M., Dijkstra P.J., Oberthür R.C., Bantjes A., Feijen J. Partially carboxymethylated feather keratins. 1. Properties in aqueous systems. Journal of Agricultural and Food Chemistry. 2000;48(9):4326–4334. doi:10.1021/jf9913155

[69] Das A., Saikia C.N. Graft copolymerization of methylmethacrylate onto non-mulberry silk-Antheraea assama using potassium permanganate–oxalic acid redox system. Bioresource Technology. 2000;74(3):213–216. doi:10.1016/S0960-8524(00)00020-1

[70] Khalil M.I., Abdel-Fattah S.H., Kantouch A. Manganese (IV)-initiated graft polymerization of vinyl monomers on polyamide fibers. Journal of Applied Polymer Science. 1975;19(10):2699–2708. doi:10.1002/app.1975.070191005

[71] Mostafa K.M. Graft polymerization of acrylic acid onto starch using potassium permanganate acid (redox system). Journal of Applied Polymer Science. 1995;56(2): 263–269. doi:10.1002/app.1995.070560217

[72] Moharana S., Mishra S.B., Tripathy S.S. Chemical modification of jute fibers. I. Permanganate-initiated graft copolymerization methyl methacrylate onto jute fibers. Journal of Applied Polymer Science. 1990;40(3–4):345–357. doi:10.1002/app.1990.070400304

[73] Zhang L.M., Chen D.Q. Grafting of 2-(Dimethylamino) ethyl methacrylate onto potato starch using potassium permanganate/sulfuric acid initiation system. Starch-Stärke. 2001;53(7):311–316. doi:10.1002/1521-379X(200107)53:7<311::AID-STAR311>3.0.CO;2-A

[74] Sarac A.S. Redox polymerization. Progress in Polymer Science. 1999;24(8):1149–1204. doi:10.1016/S0079-6700(99)00026-X

[75] Martinez-Hernandez A.L., Velasco-Santos C., Icaza M.D., Castaño V.M. Grafting of methyl methacrylate onto natural keratin. e-Polymers. 2003;3(1):209–219. doi:10.1515/epoly.2003.3.1.209

[76] Jyothi A.N., Carvalho A.J.F. Starch-g-copolymers: synthesis, properties and applications. In: Kalia S., Sabaa M.W., editors. Polysaccharide based graft copolymers. Berlin Heidelberg: Springer; 2013. p. 59–109. doi:10.1007/978-3-642-36566-9_3

[77] Martínez-Hernández A.L., Santiago-Valtierra A.L., Alvarez-Ponce M.J. Chemical modification of keratin biofibres by graft polymerisation of methyl methacrylate using redox initiation. Materials Research Innovations. 2008;12(4):184–191. doi:http://dx.doi.org/10.1179/143307508X362828

[78] Shon C.H., Gao J., Thomas D.A., Kim T.-Y., Goddard III W.A., Beauchamp J.L. Mechanisms and energetics of free radical initiated disulfide bond cleavage in model peptides and insulin by mass spectrometry. Chemical Science. 2015;6(8):4550–4560. doi:10.1039/C5SC01305D

[79] Fuhrmann J., Clancy K.W., Thompson P.R. Chemical biology of protein arginine modifications in epigenetic regulation. Chemical Reviews. 2015;115(11):5413–5461. doi: 10.1021/acs.chemrev.5b00003

[80] Aljawish A., Chevalot I., Jasniewski J., Scher J., Muniglia L. Enzymatic synthesis of chitosan derivatives and their potential applications. Journal of Molecular Catalysis B: Enzymatic. 2015;112:25–39. doi:10.1016/j.molcatb.2014.10.014

[81] Kim S.-K., Medis E. Bioactive compounds from marine processing byproducts – a review. Food Research International. 2006;39(4):383–393. doi:10.1016/j.foodres. 2005.10.010

[82] Hejazi R., Amiji M. Chitosan-based gastrointestinal delivery systems. Journal of Controlled Release. 2003;89:151–165. doi:10.1016/S0168-3659(03)00126-3

[83] Dash M., Chiellini F., Ottenbrite R.M., Chiellini E. Chitosan—A versatile semi-synthetic polymer in biomedical applications. Progress in Polymer Science. 2011;36(8):981–1014. doi:10.1016/j.progpolymsci.2011.02.001

[84] Xu G., Shi T., Li M., Yu F., Chen Y. Difference between the effects of modification graphene oxide with two biomass molecules: chitosan and cardanol. Research on Chemical Intermediates. 2015;41(11):8499–8513. doi:10.1007/s11164-014-1906-0

[85] Yang Q., Pan X., Clarket K., Li K. Covalent Functionalization of Graphene with Polysaccharides. Industrial & Engineering Chemistry Research. 2012;51(1):310–317. doi:10.1021/ie201391e

[86] Shao L., Chang X., Zhang Y., Huang Y., Yao Y., Guo Z. Graphene oxide cross-linked chitosan nanocomposite membrane. Applied Surface Science. 2013;280:989–992. doi: 10.1016/j.apsusc.2013.04.112

[87] Wang J., Gao X., Wang J., Wei Y., Li Z., Gao C. O-(carboxymethyl)-chitosan nanofiltration membrane surface functionalized with graphene oxide nanosheets for enhanced desalting properties. ACS Applied Materials & Research. 2015;7(7):4381–4389. doi: 10.1021/am508903g

[88] Singh A., Sinsinbar G., Choudhary M., Kumar V., Pasricha R., Verma H.N., et al. Graphene oxide-chitosan nanocomposite based electrochemical DNA biosensor for detection of typhoid. Sensors and Actuators B: Chemical. 2013;185:675–684. doi: 10.1016/j.snb.2013.05.014

[89] Rana V.K., Choi M.-C., Kong J.-Y., Kim M.J., Kim S.-H., Mishra S., et al. Synthesis and drug-delivery behavior of chitosan-functionalized graphene oxide hybrid nanosheets. Macromolecular Materials and Engineering. 2011;296(2):131–140. doi:10.1002/mame. 201000307

[90] Bao H., Pan Y., Ping Y., Sahoo N.G., Wu T., Li L., et al. Chitosan-functionalized graphene oxide as a nanocarrier for drug and gene delivery. Small. 2011;7(11):1569–1578. doi:10.1002/smll.201100191

[91] Depan D., Pesacreta T.C., Misra R.D.K. The synergistic effect of a hybrid graphene oxide–chitosan system and biomimetic mineralization on osteoblast functions. Biomaterials Science. 2014;2(2):264–274. doi:10.1039/C3BM60192G

[92] Wang J., Zhao G., Jing L., Peng X., Li Y. Facile self-assembly of magnetite nanoparticles on three-dimensional graphene oxide–chitosan composite for lipase immobilization. Biochemical Engineering Journal. 2015;98:75–83. doi:10.1016/j.bej.2014.11.013

[93] Zuo P.-P., Feng H.-F., Xu Z.-Z., Zhang L.-F., Zhang Y.-L., Xia W., Zhang W.-Q. Fabrication of biocompatible and mechanically reinforced graphene oxide-chitosan nanocomposite films. Chemistry Central Journal. 2013;7(39). doi:10.1186/1752-153X-7-39

[94] Justin R., Chen B. Strong and conductive chitosan–reduced graphene oxide nanocomposites for transdermal drug delivery. Journal of Materials Chemistry B. 2014;2(24): 3759–3770. doi:10.1039/C4TB00390J

[95] Depan D., Girase B., Shah J.S., Misra R.D.K. Structure–process–property relationship of the polar graphene oxide-mediated cellular response and stimulated growth of osteoblasts on hybrid chitosan network structure nanocomposite scaffolds. Acta Biomaterialia. 2011;7(9):3432–3445. doi:10.1016/j.actbio.2011.05.019

[96] Mohandes F., Salavati-Niasara M. Freeze-drying synthesis, characterization and in vitro bioactivity of chitosan/graphene oxide/hydroxyapatite nanocomposite. RSC Advances. 2014;4(49):25993–26001. doi:10.1039/C4RA03534H

[97] Li L., Luo C., Li X., Duan H., Wang X. Preparation of magnetic ionic liquid/chitosan/graphene oxide composite and application for water treatment. International Journal of Biological Macromolecules. 2014;66:172–178. doi:10.1016/j.ijbiomac.2014.02.031

[98] Fan L., Luo C., Li X., Lu F., Qiu H., Sun M. Fabrication of novel magnetic chitosan grafted with graphene oxide to enhance adsorption properties for methyl blue. Journal of Hazardous Materials. 2012;215–216:272–279. doi:10.1016/j.jhazmat.2012.02.068

[99] Li L., Fan L., Luo C., Duan H., Wang X. Study of fuchsine adsorption on magnetic chitosan/graphene oxide. RSC Advances. 2014;4(47):24. doi:24679–24685

[100] Hegab H.M., Wimalasiri Y., Ginic-Markovic, Zou L. Improving the fouling resistance of brackish water membranes via surface modification with graphene oxide functionalized chitosan. Desalination. 2015;365:99–107. doi:10.1016/j.desal.2015.02.029

[101] Cheng W., Wang M., Yang Z., Sun Y., Ding C. The efficient enrichment of U(VI) by graphene oxide-supported chitosan. RSC Advances. 2014;4(106):61919–61926. doi: 10.1039/C4RA09541C

[102] Maleki A., Paydar R. Graphene oxide–chitosan bionanocomposite: a highly efficient nanocatalyst for the one-pot three-component synthesis of trisubstituted imidazoles under solvent-free conditions. RSC Advances. 2015;5(42):33177–33184. doi:10.1039/C5RA03355A

[103] Rajesh R., Sujanthi E., Kumar S.S., Venkatesan R. Designing versatile heterogeneous catalysts based on Ag and Au nanoparticles decorated on chitosan functionalized graphene oxide. Physical Chemistry Chemical Physics. 2015;17(17):11329–11340. doi: 10.1039/C5CP00682A

[104] Liao K.-H., Lin Y.-S., Macosko C.W., Haynes C.L. Cytotoxicity of graphene oxide and graphene in human erythrocytes and skin fibroblasts. ACS Applied Materials & Interfaces. 2011;3(7):2607–2615. doi:10.1021/am200428v

[105] Ling Y., Li X., Zhou S., Wang X., Sun R. Multifunctional cellulosic paper based on quaternized chitosan and gold nanoparticle–reduced graphene oxide via electrostatic self-assembly. Journal of Materials Chemistry A. 2015;3(14):7422–7428. doi:10.1039/C4TA07160C

[106] Song Y., Liu H., Tan H., Xu F., Jia J., Zhang L., et al. pH-Switchable electrochemical sensing platform based on chitosan-reduced graphene oxide/concanavalin a layer for assay of glucose and urea. Analytical Chemistry. 2014;86(4):1980–1987. doi:10.1021/ac402742m

[107] Li X., Zhou H., Wu W., Wei S., Xu Y., Kuang Y. Studies of heavy metal ion adsorption on Chitosan/Sulfydryl-functionalized graphene oxide composites. Journal of Colloid and Interface Science. 2015;448:389–397. doi:10.1016/j.jcis.2015.02.039

[108] Gruskiene R., Deveikyte R. Ricardas M. Quaternization of chitosan and partial destruction of the quaternized derivatives making them suitable for electrospinning. CHEMIJA. 2013;24(4):325–334.

[109] Han D., Xiao P., Gu J., Chen J., Cai Z., Zhang J., et al. Polymer brush functionalized Janus graphene oxide/chitosan hybrid membranes. RSC Advances. 2014;4(43):22759–22762. doi:10.1039/C4RA02826K

[110] Pan Y., Wu T., Bao H., Li L. Green fabrication of chitosan films reinforced with parallel aligned graphene oxide. Carbohydrate Polymers. 2011;83(4):1908–1915. doi:10.1016/j.carbpol.2010.10.054

[111] Justin R., Chen B. Characterisation and drug release performance of biodegradable chitosan–graphene oxide nanocomposites. Carbohydrate Polymers. 2014;103:70–80. doi:10.1016/j.carbpol.2013.12.012

[112] Sayyar S., Murray E., Thompson B.C., Chung J., Officer D.L., Gambhir S., et al. Processable conducting graphene/chitosan hydrogels for tissue engineering. Journal of Materials Chemistry B. 2015;3(3):481–490. doi:10.1039/C4TB01636J

[113] Han D., Yan L. Supramolecular hydrogel of chitosan in the presence of graphene oxide nanosheets as 2D cross-linkers. ACS Sustainable Chemistry & Engineering. 2014;2(2):296–300. doi:10.1021/sc400352a

[114] Wei H., Han L., Tang Y., Ren J., Zhao Z., Jia L. Highly flexible heparin-modified chitosan/graphene oxide hybrid hydrogel as a super bilirubin adsorbent with excellent

hemocompatibility. Journal of Materials Chemistry B. 2015;3(8):1646–1654. doi:10.1039/C4TB01673D

[115] He L., Wang H., Xia G., Sun J., Song R. Chitosan/graphene oxide nanocomposite films with enhanced interfacial interaction and their electrochemical applications. Applied Surface Science. 2014;314:510–515. doi:10.1016/j.apsusc.2014.07.033

[116] Abdelhamid H.N., Wu H.-F. Multifunctional graphene magnetic nanosheet decorated with chitosan for highly sensitive detection of pathogenic bacteria. Journal of Materials Chemistry B. 2013;1(32):3950–3961. doi:10.1039/C3TB20413H

[117] Luo Z., Yang D., Qi G., Yuwen L., Zhang Y., Weng L., et al. Preparation of highly dispersed reduced graphene oxide decorated with chitosan oligosaccharide as electrode material for enhancing the direct electron transfer of *Escherichia coli*. ACS Applied Materials & Interfaces. 2015;7(16):8539–8544. doi:10.1021/acsami.5b00297

[118] Li M., Wang Y., Liu Q., Li Q., Cheng Y., Zheng Y., et al. In situ synthesis and biocompatibility of nano hydroxyapatite on pristine and chitosan functionalized graphene oxide. Journal of Materials Chemistry B. 2013;1(4):475–484. doi:10.1039/C2TB00053A

[119] Feng X., Wang X., Xing W., Yu B., Song L., Hu Y. Simultaneous reduction and surface functionalization of graphene oxide by chitosan and their synergistic reinforcing effects in PVA films. Industrial & Engineering Chemistry Research. 2013;52(36):12906–12914. doi:10.1021/ie402073x

[120] Ko T.Y., Kim S.Y., Kim H.G., Moon G.-S., In I. Antibacterial activity of chemically reduced graphene oxide assembly with chitosan through noncovalent interactions. Chemistry Letters. 2013;42:66–67. doi:http://doi.org/10.1246/cl.2013.66

[121] Pan Y., Bao H., Li L. Noncovalently functionalized multiwalled carbon nanotubes by chitosan-grafted reduced graphene oxide and their synergistic reinforcing effects in chitosan films. ACS Applied Materials & Interfaces. 2011;3(12):4819–4830. doi:10.1021/am2013135

[122] Yang X., Tu Y., Li L., Shang S., Tao X.-m. Well-dispersed chitosan/graphene oxide nanocomposites. ACS Applied Materials & Interfaces. 2010;2(6):1707–1713. doi:10.1021/am100222m